



Overview of STAR-BES results

Lijuan Ruan (BNL)

July 21, 2025

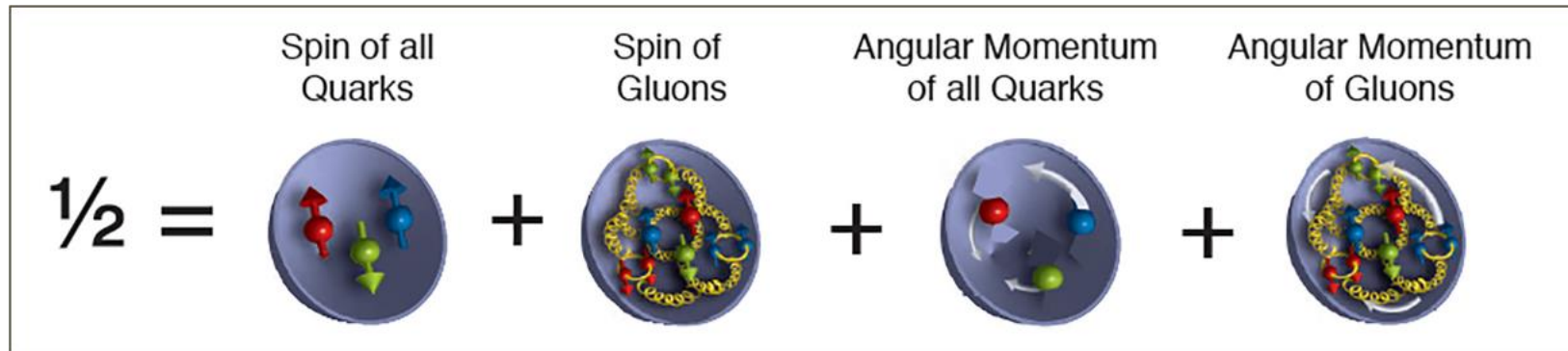
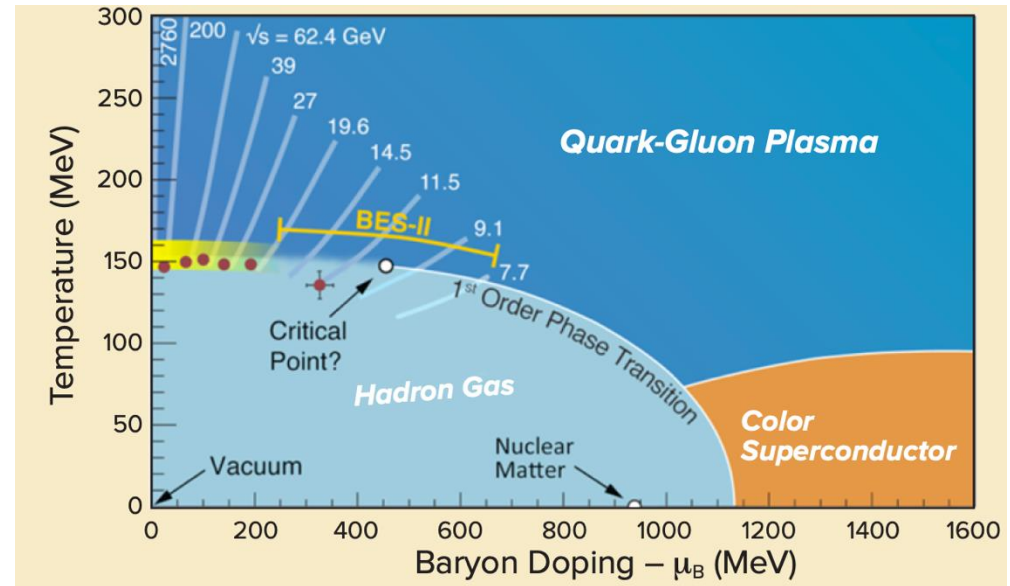
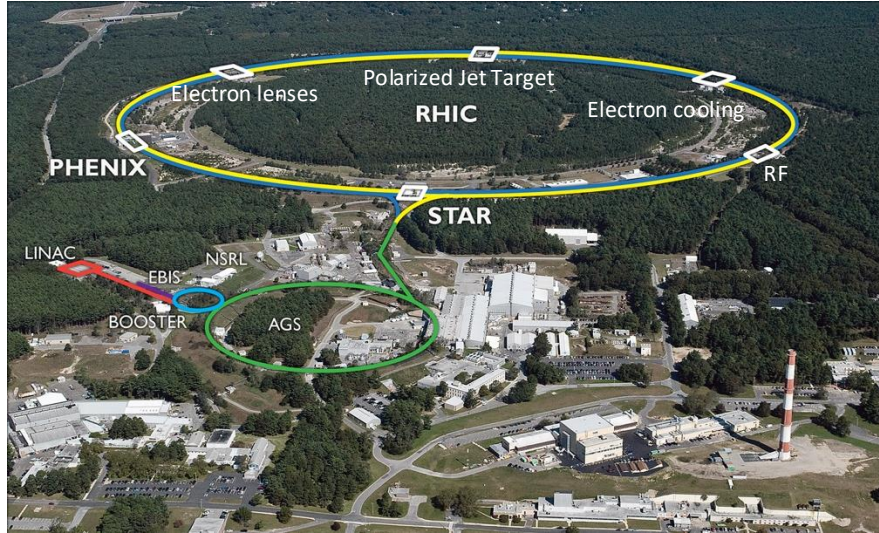


RHIC @ Brookhaven National Laboratory



25 years of RHIC operation

The mission of RHIC



To probe the inner workings of the Quark-Gluon Plasma

To map the phase diagram of QCD

To study the spin puzzle of proton

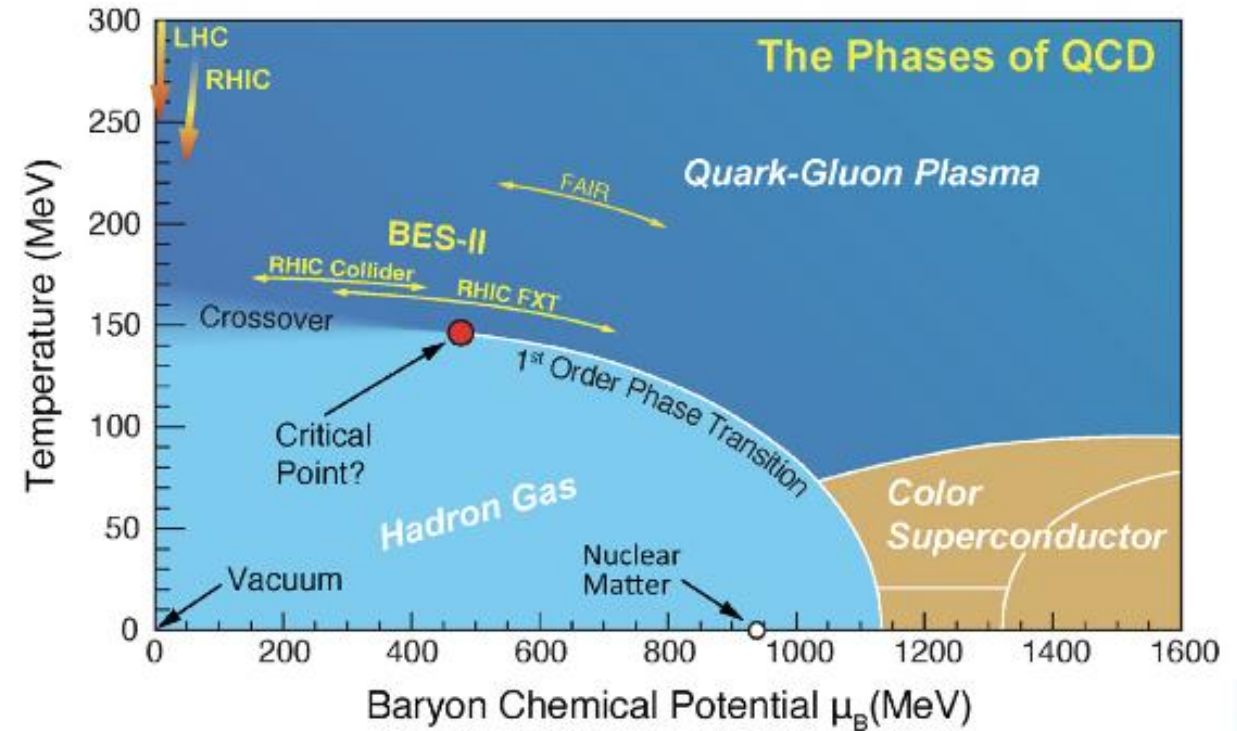
The phases of QCD matter

Lattice QCD: crossover chiral transition at $\mu_B < 3 \text{ T}$

At top RHIC and LHC energies, measurements consistent with a smooth crossover chiral transition

Change T and μ_B by varying the collision energy:

- Search for the critical point
- Search for the first-order phase transition
- Search for the threshold of QGP formation



STAR beam energy scan phase I campaign



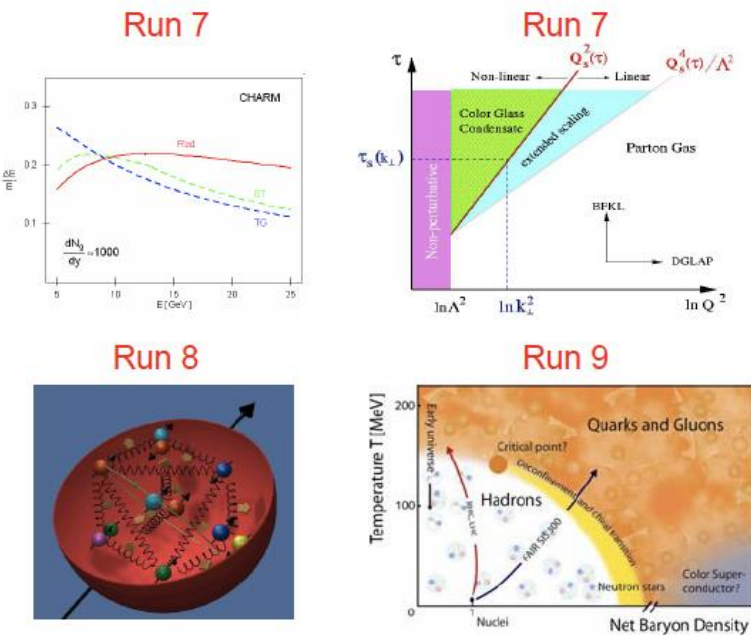
STAR Multi-Year Beam Use Request For

In 2006, stated in the Beam Use Request:
definite search for the existence and location of the
QCD Critical Point for Run 2009

RHIC Beam Energy Scan Phase I in 2010 and 2011

Energy (GeV)	7.7	11.5	19.6	27	39	62.4	200
Statistics (Million)	~3	~6.6	~15	~30	~87	~47	~242
Year	2010	2010	2011	2011	2010	2010	2010

Time of flight detector upgrade, DAQ1000
just completed before Run 2010



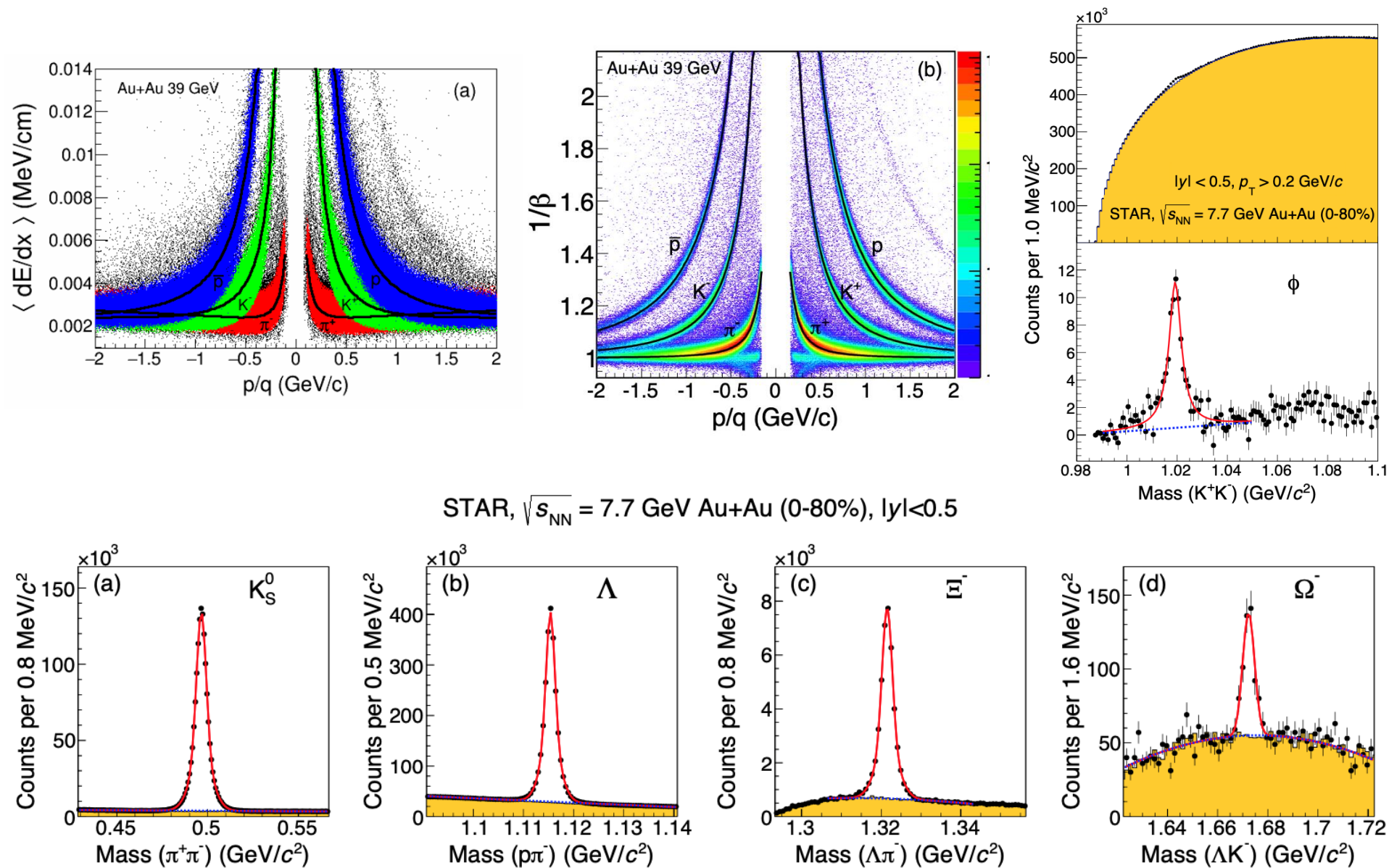
Tim Hallman for the STAR Collaboration

Brookhaven National Laboratory
September 12, 2006

Hallman, BNL PAC, 9/12/2006

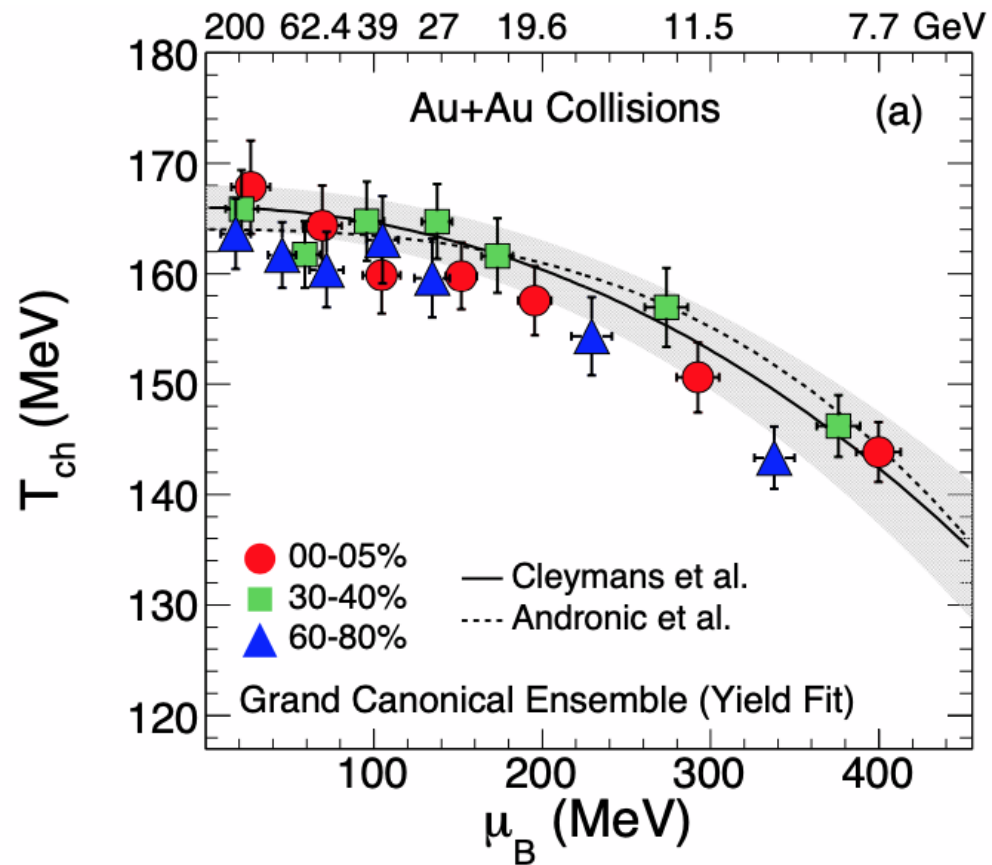


Particle identification with TPC+TOF



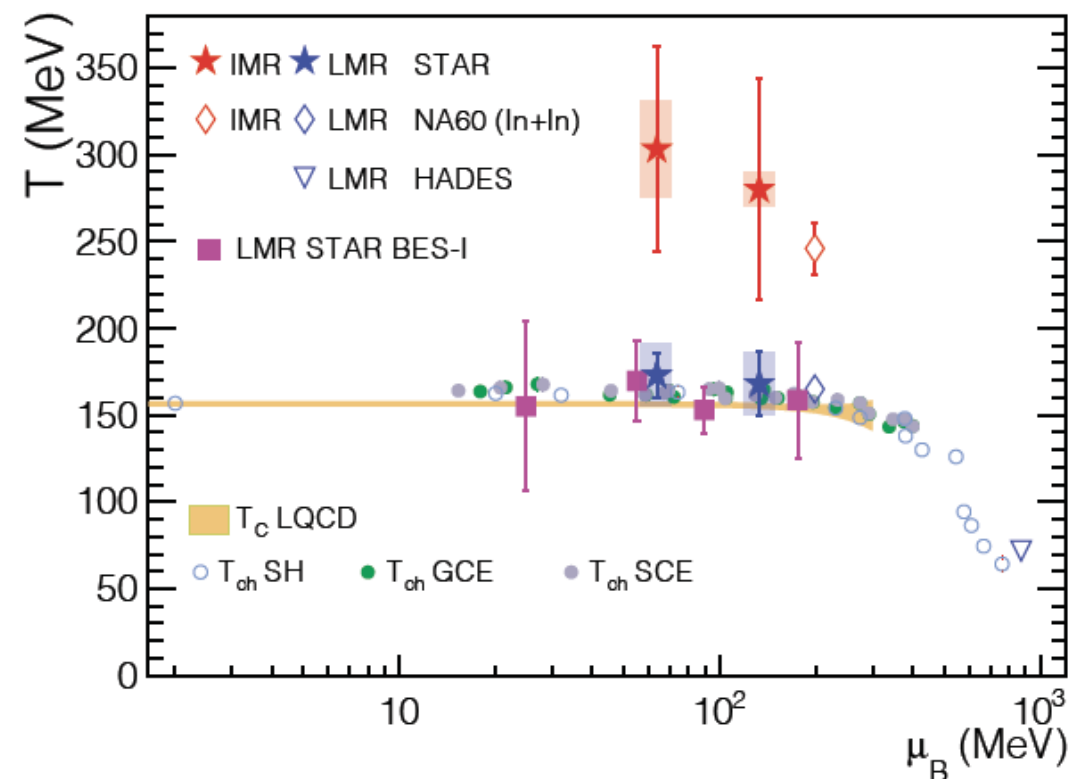
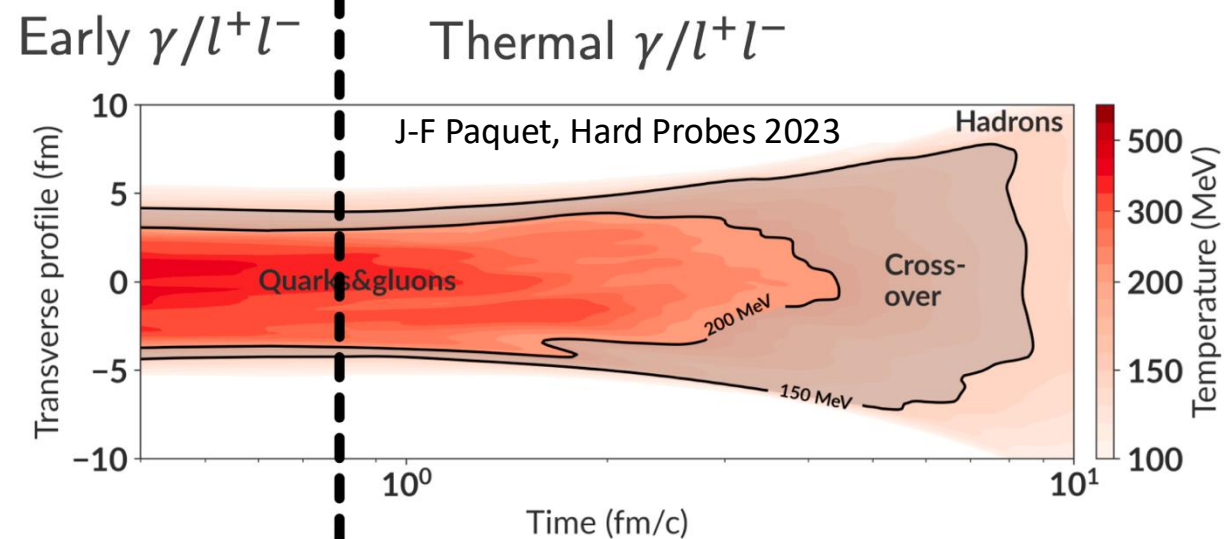
Locate T and μ_B

Phys. Rev. C 96 (2017) 44904



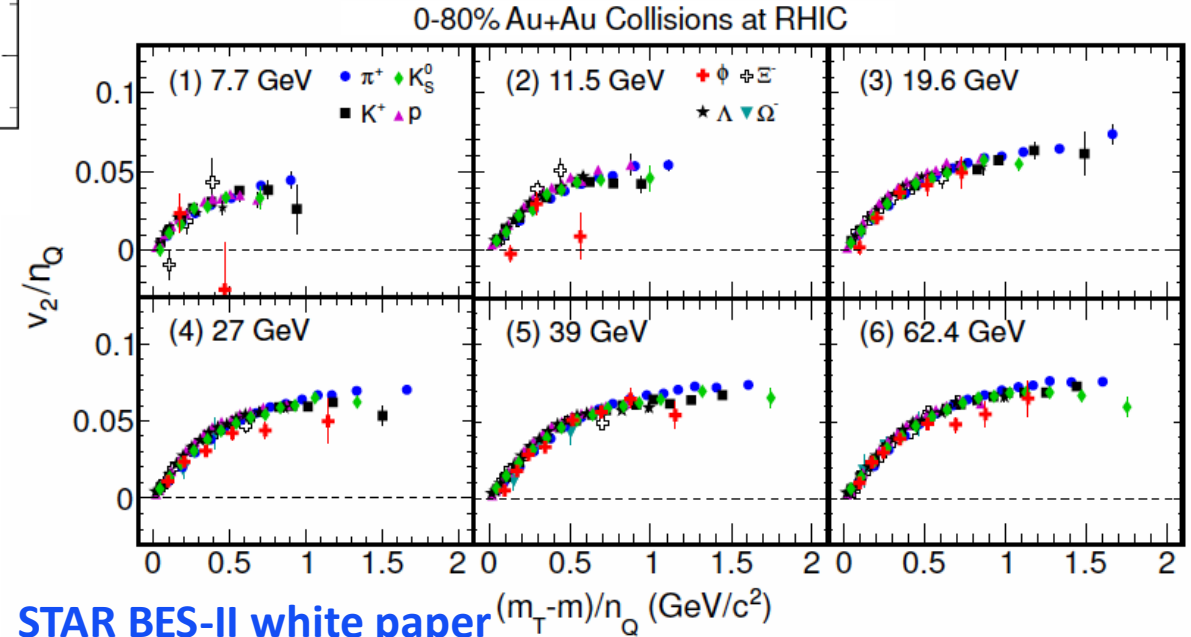
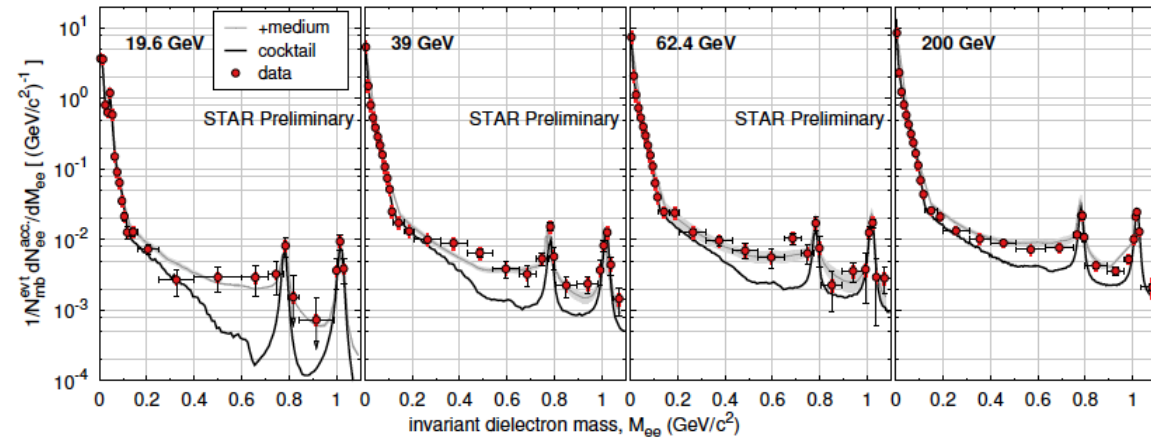
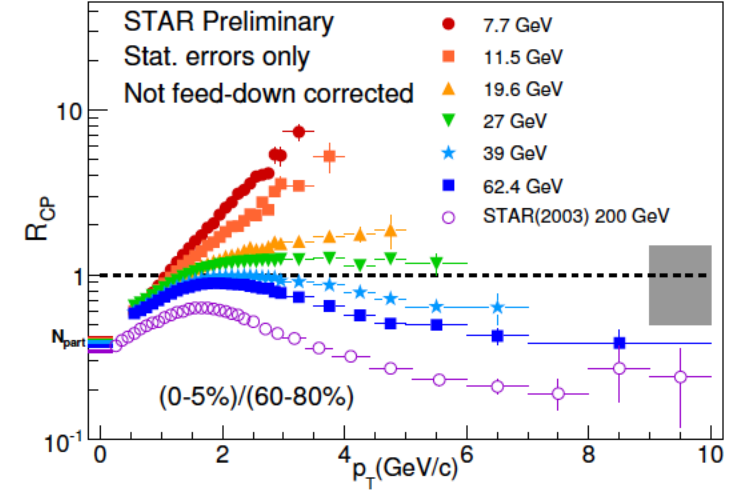
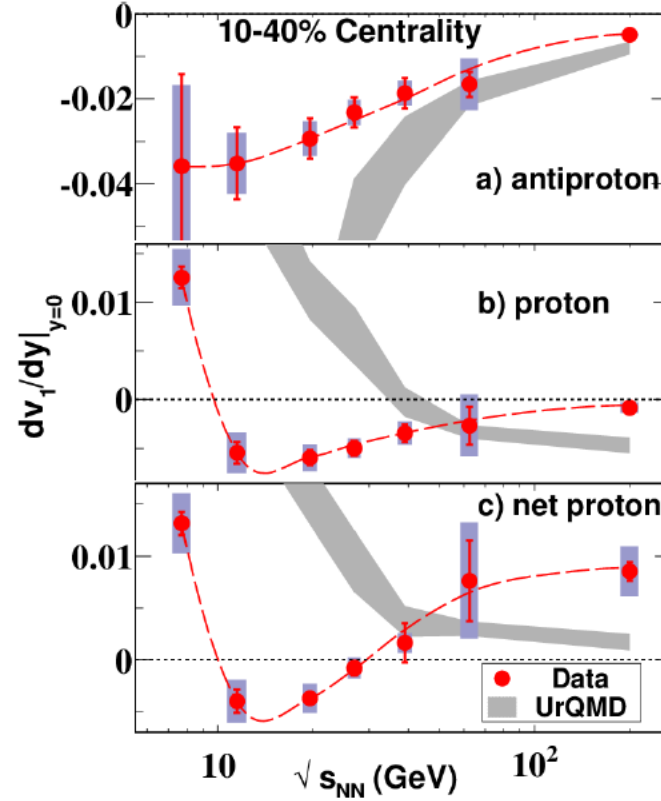
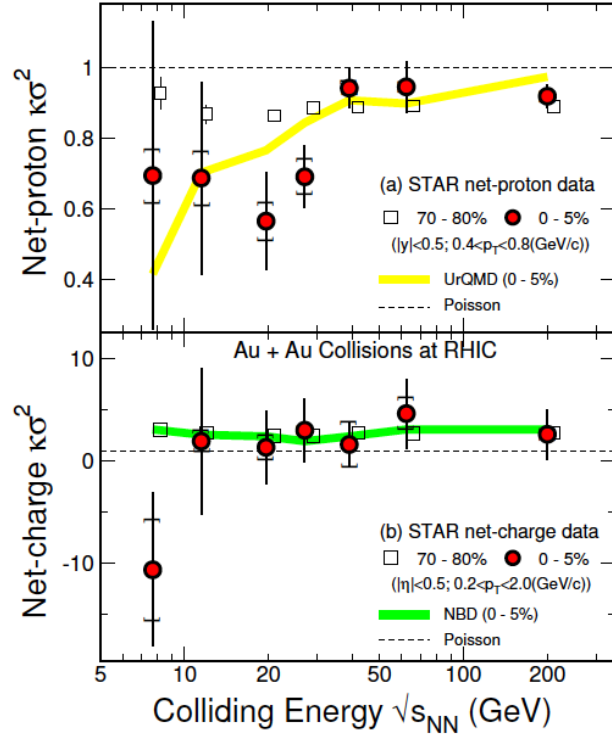
$\pi^\pm, K^\pm, p, \bar{p}, \Lambda, \bar{\Lambda}, \Xi, \text{ and } \bar{\Xi}.$

$\pi^-/\pi^+, \bar{K}^-/K^+, \bar{p}/p, \bar{\Lambda}/\Lambda, \bar{\Xi}/\Xi, K^-/\pi^-, \bar{p}/\pi^-, \Lambda/\pi^-,$
and $\bar{\Xi}/\pi^-.$



arXiv: 2402.01998, submitted to Nature Communications

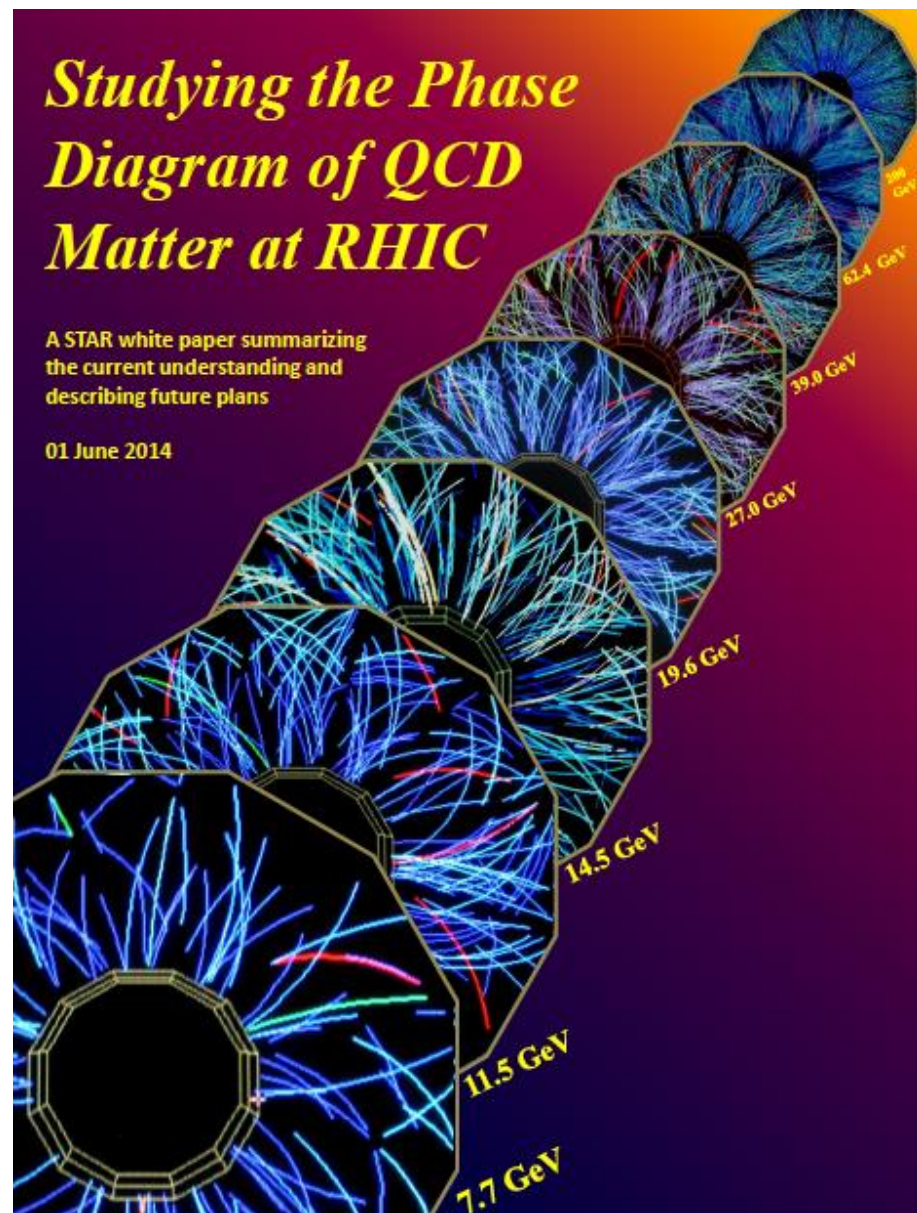
Selected results from BES-I



STAR beam energy scan phase II campaign

STAR Collaboration Decadal Plan December 2010

1 Executive Summary	3
2 What is the nature of QCD matter at the extremes?	8
2.1 What are the properties of the strongly-coupled system produced at RHIC, and how does it thermalize?	9
2.1.1 What do we know now and what do we want to know further?	9
2.1.2 What measurements do we need?	16
2.2 What is the detailed mechanism for partonic energy loss?	29
2.2.1 What do we know now?	29
2.2.2 What measurements do we need to perform to answer the question?	34
2.3 Where is the QCD critical point and the associated first-order phase transition line?	46
2.3.1 Status of the QCD Phase Diagram	46
2.3.2 Search for the QCD Critical Point and Phase Transition Line	49
2.3.3 Advantages of RHIC/STAR	53
2.3.4 Next steps	55
2.4 Can we strengthen current evidence for novel symmetries in QCD matter and open new avenues?	56
2.4.1 Local Parity Violation	56
2.4.2 Dilepton measurements and chiral symmetry restoration	59
2.4.3 Rare Decays	62
2.5 What other exotic particles are created at RHIC?	66
2.5.1 Discoveries of the heaviest antimatter and antihypernuclei	66
2.5.2 Glueball search	71
2.5.3 Searches for di-baryon states with the STAR detector	74
3 What is the partonic structure of nucleons and nuclei?	77
3.1 What is the partonic spin structure of the proton?	78
3.1.1 Gluon Polarization	78
3.1.2 Quark Polarization	82
3.1.3 Quark Transversity	87
3.2 How do we go beyond leading twist and collinear factorization in perturbative QCD?	92
3.2.1 Transverse spin asymmetries	92



STAR beam energy scan phase II campaign

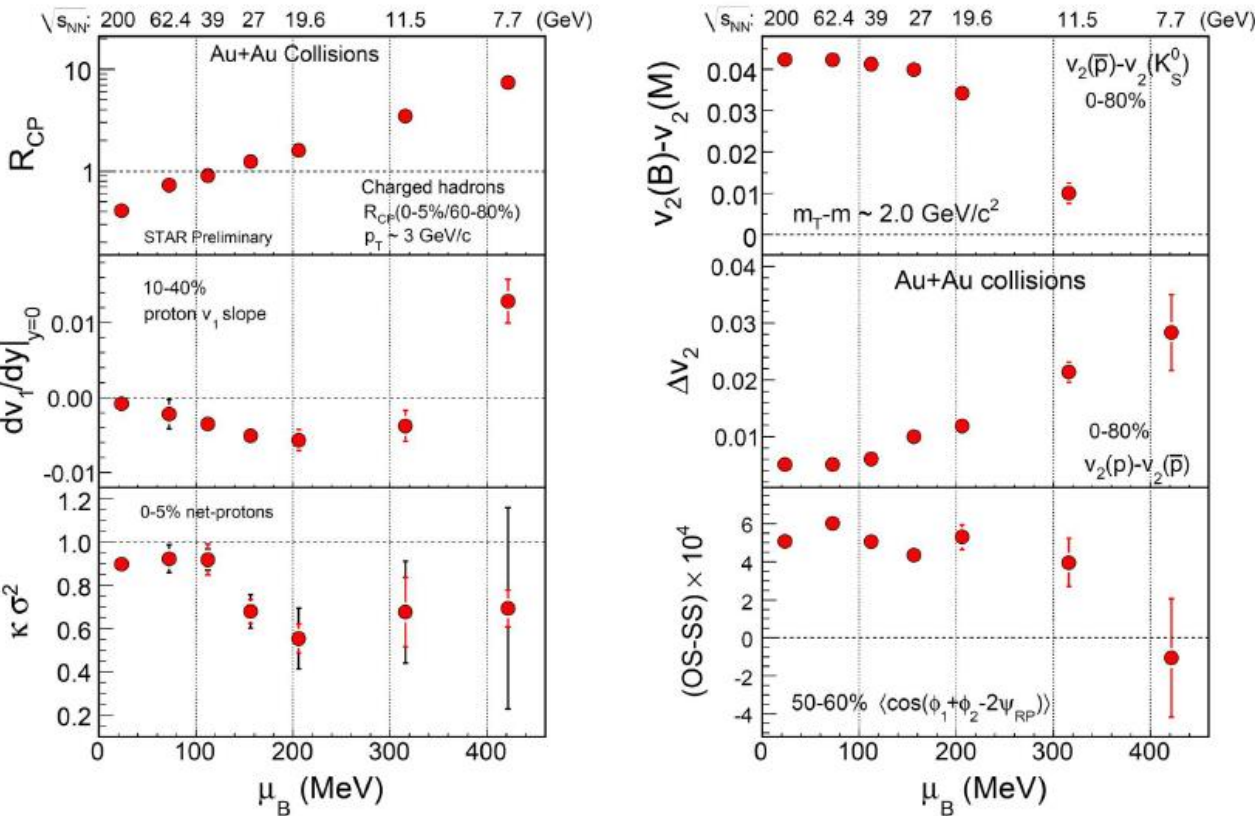
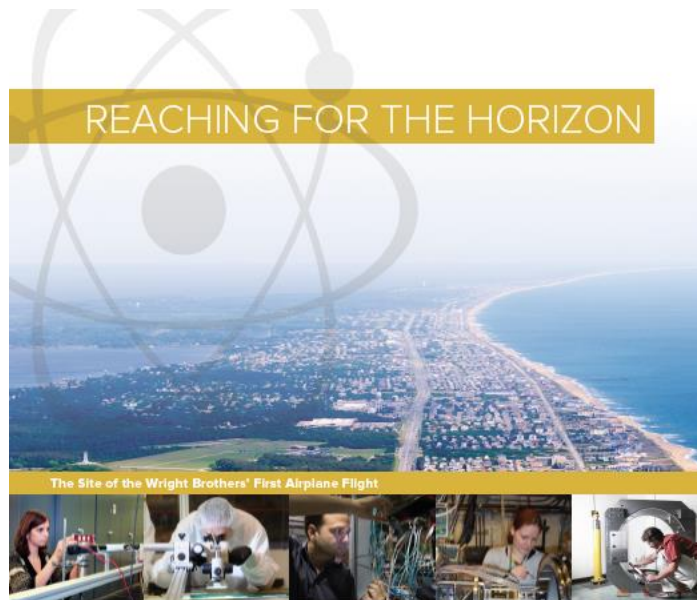


Table 2. Event statistics (in millions) needed for Beam Energy Scan Phase-II for various observables.

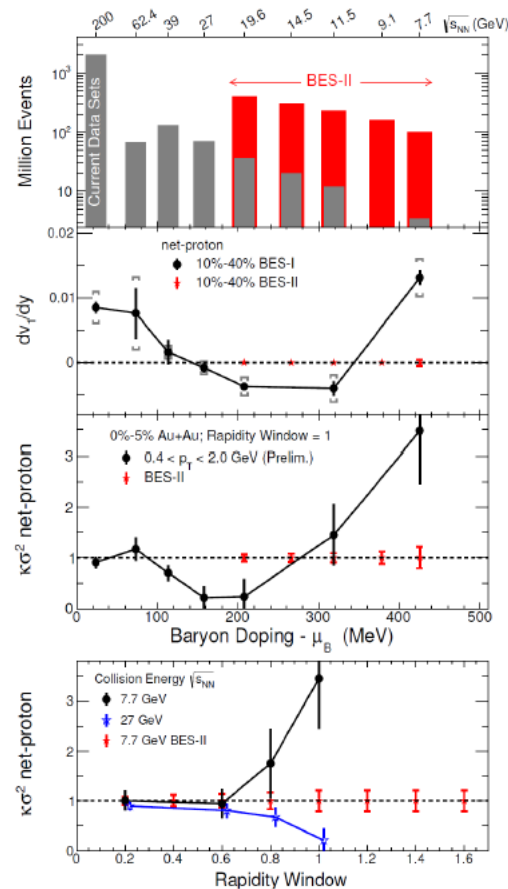
Collision Energy (GeV)	7.7	9.1	11.5	14.5	19.6
μ_B (MeV) in 0-5% central collisions	420	370	315	260	205
Observables					
R_{CP} up to $p_T = 5$ GeV/c	–		160	125	92
Elliptic Flow (ϕ mesons)	100	150	200	200	400
Chiral Magnetic Effect	50	50	50	50	50
Directed Flow (protons)	50	75	100	100	200
Azimuthal Femtoscopy (protons)	35	40	50	65	80
Net-Proton Kurtosis	80	100	120	200	400
Dileptons	100	160	230	300	400
Required Number of Events	100	160	230	300	400

<https://drupal.star.bnl.gov/STAR/starnotes/public/sn0598>

The 2015 long range plan for nuclear science



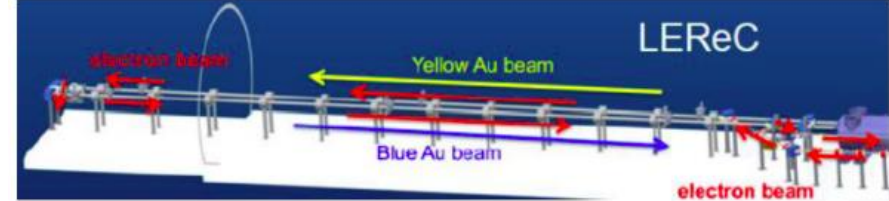
The 2015 LONG RANGE PLAN for NUCLEAR SCIENCE



2015 LRP:

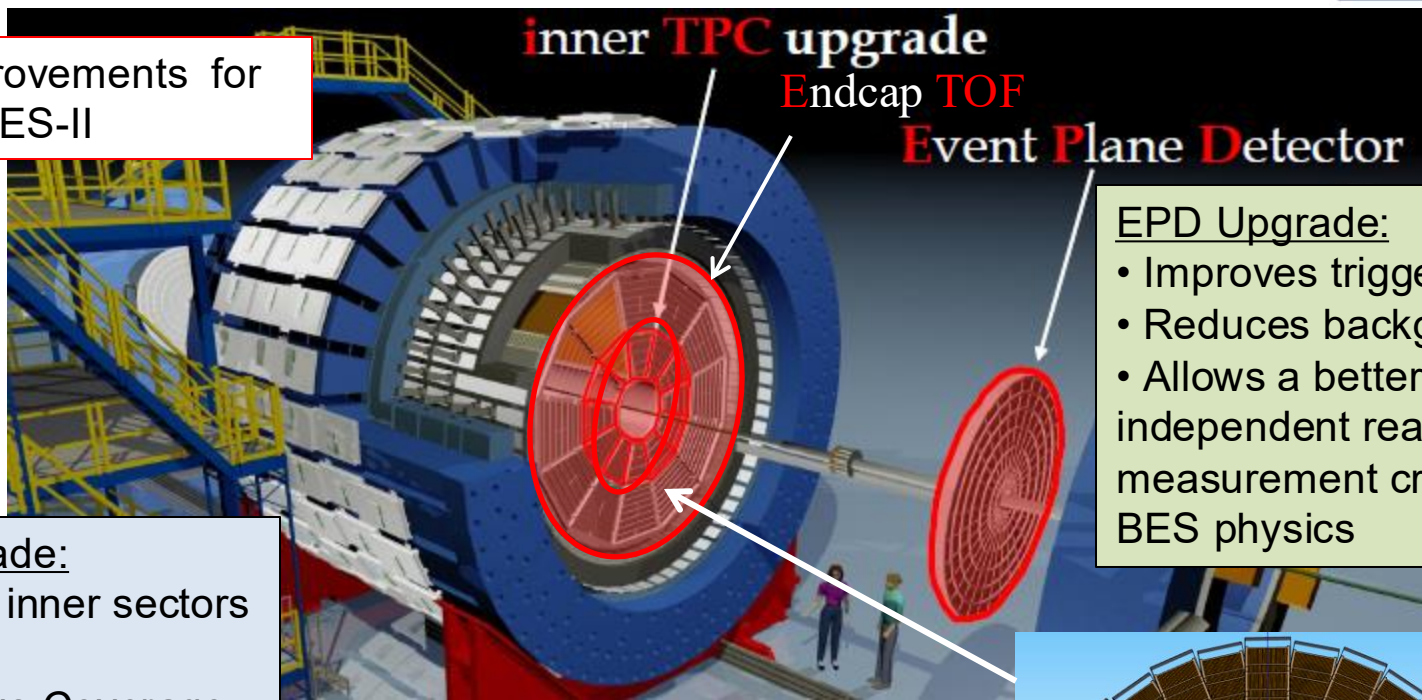
“There are two central goals of measurements planned at RHIC, as it completes its scientific mission, and at the LHC: **(1) Probe the inner workings of QGP by resolving its properties at shorter and shorter length scales. The complementarity of the two facilities is essential to this goal, as is a state-of-the-art jet detector at RHIC, called sPHENIX. (2) Map the phase diagram of QCD with experiments planned at RHIC.**”

RHIC BES-II upgrades



LEReC – Low Energy RHIC electron Cooling

Major improvements for
BES-II



iTPC Upgrade:

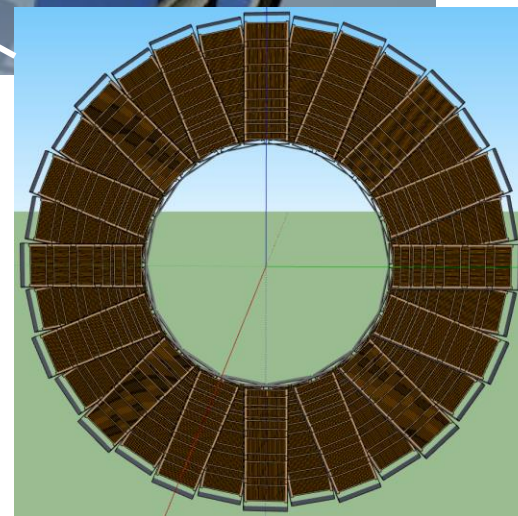
- Replaced inner sectors of the TPC
- Continuous Coverage
- Improves dE/dx
- Extends η coverage from 1.0 to 1.5
- Lowers p_T cut from 125 MeV/c to 60 MeV/c

EPD Upgrade:

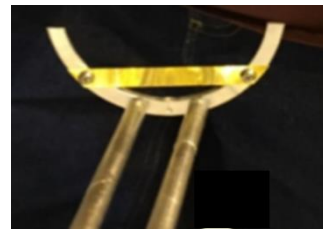
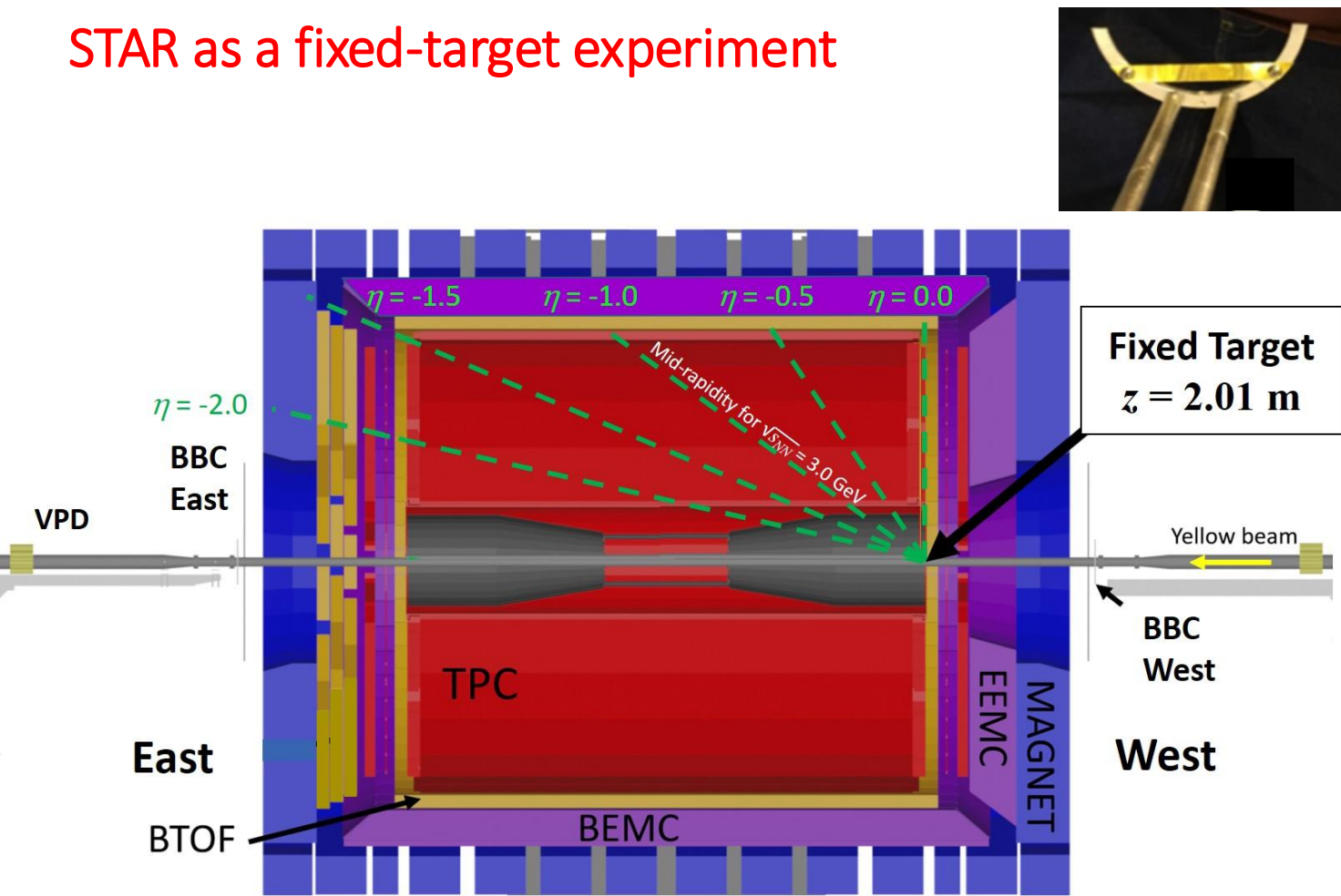
- Improves trigger
- Reduces background
- Allows a better and independent reaction plane measurement critical to BES physics

EndCap TOF Upgrade:

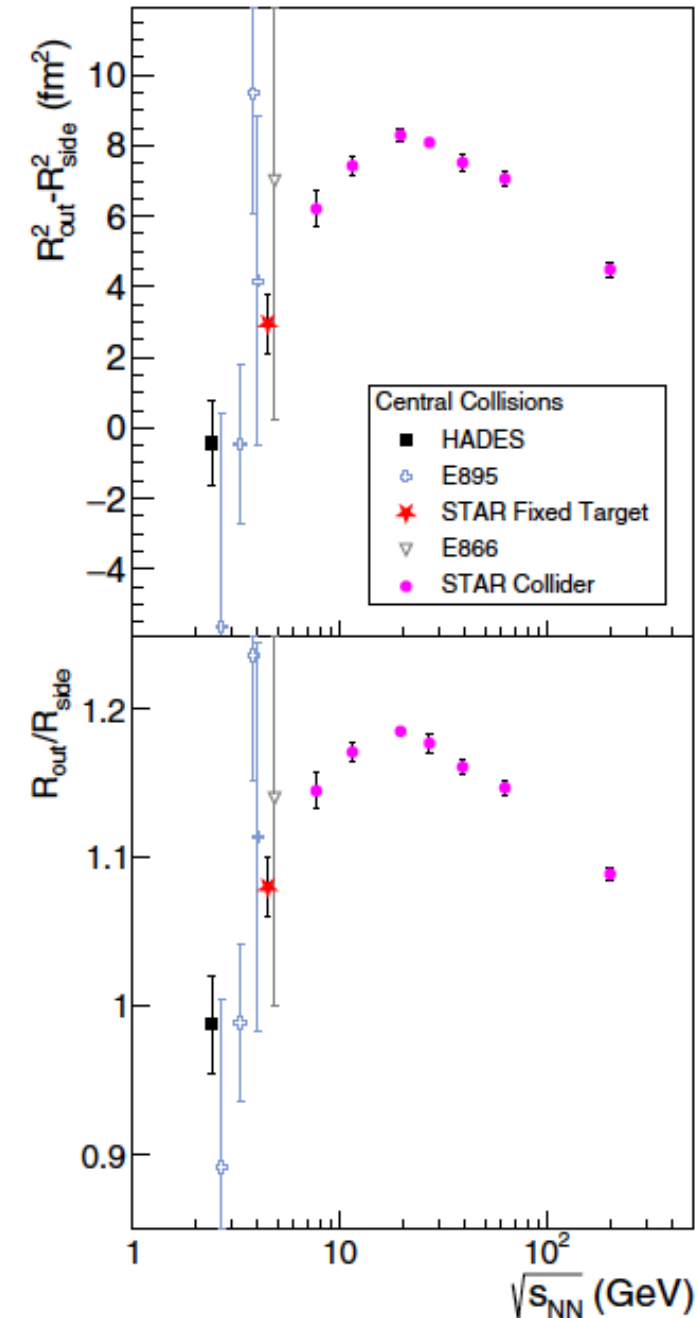
- Rapidity coverage is critical
- PID at $\eta = 1$ to 1.5
- Improves the fixed target program
- Provided by CBM-FAIR



STAR as a fixed-target experiment



Phys. Rev. C **103** (2021) 034908



A gold target was installed inside the beam pipe in December 2013 for a feasibility test

- collected data during 14.5 GeV Run in 2014

A thinner gold target was installed for FXT program 2018-2021

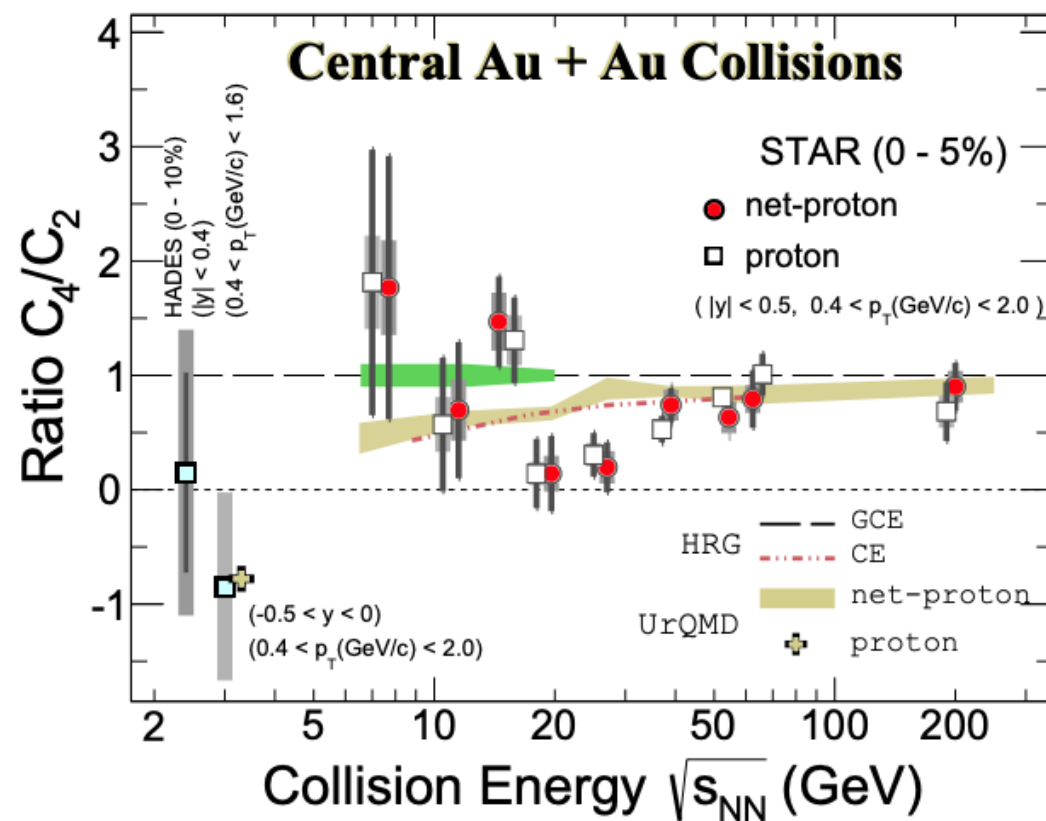
BES-II datasets (2019-2021)

Au+Au Collisions at RHIC							
Collider Runs				Fixed-Target Runs			
	$\sqrt{s_{NN}}$ (GeV)	#Events	μ_B		$\sqrt{s_{NN}}$ (GeV)	#Events	μ_B
1	200	380 M	25 MeV	1	13.7 (100)	50 M	280 MeV
2	62.4	46 M	75 MeV	2	11.5 (70)	50 M	316 MeV
3	54.4	1200 M	85 MeV	3	9.2 (44.5)	50 M	372 MeV
4	39	86 M	112 MeV	4	7.7 (31.2)	260 M	420 MeV
5	27	585 M	156 MeV	5	7.2 (26.5)	470 M	440 MeV
6	19.6	595 M	206 MeV	6	6.2 (19.5)	120 M	490 MeV
7	17.3	256 M	230 MeV	7	5.2 (13.5)	100 M	540 MeV
8	14.6	340 M	262 MeV	8	4.5 (9.8)	110 M	590 MeV
9	11.5	257 M	316 MeV	9	3.9 (7.3)	120 M	633 MeV
10	9.2	160 M	372 MeV	10	3.5 (5.75)	120 M	670 MeV
11	7.7	104 M	420 MeV	11	3.2 (4.59)	200 M	699 MeV
				12	3.0 (3.85)	260 + 2000 M	750 MeV

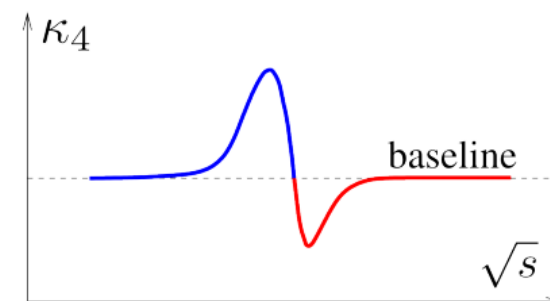
A broad μ_B coverage: $25 < \mu_B < 750$ MeV

BES-II data collected at RHIC cover a broad and interesting range of μ_B for the critical point search

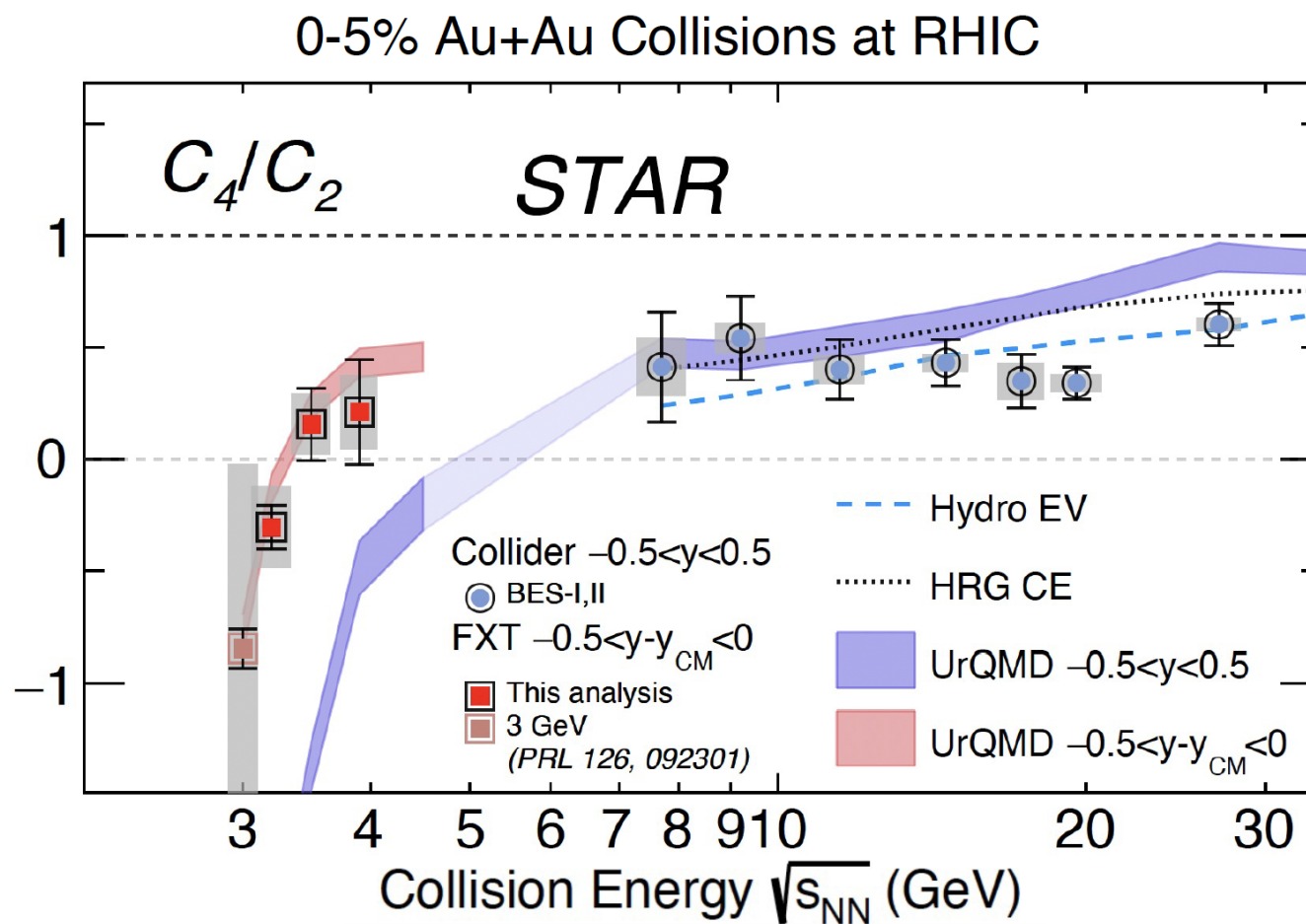
Net-proton higher moments from BES-I and at 3 GeV from FXT (2018)



BES-I: PRL 126 (2021) 092301
 3 GeV data: PRL 128 (2022) 202303



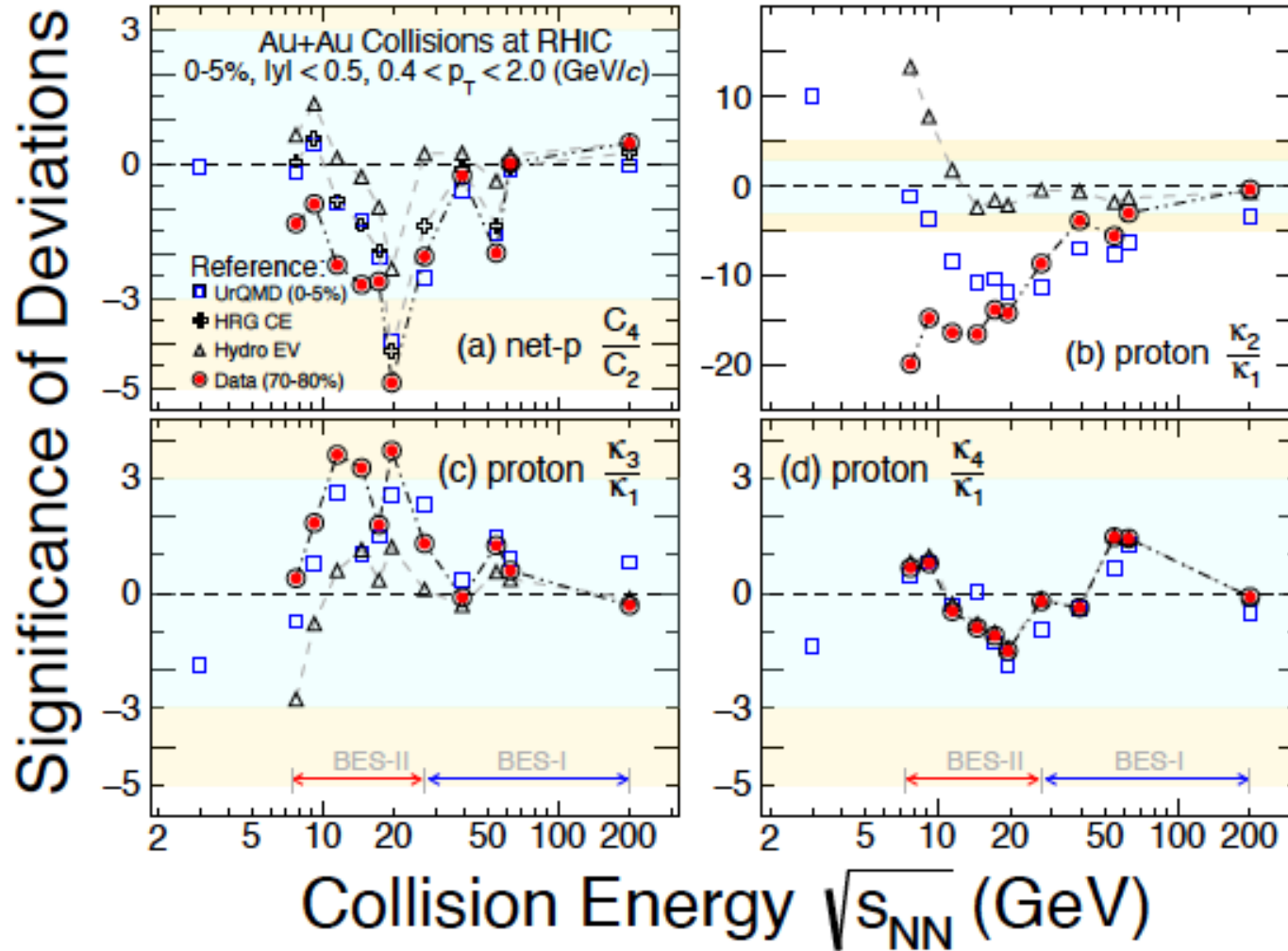
- Non-monotonic energy dependence in central Au+Au collisions (3.1σ)
- Strong suppression in proton C_4/C_2 at 3 GeV
 - consistent with UrQMD hadronic transport model calculation



Net-proton cumulants and proton factorial cumulants from 7.7 GeV to 27 GeV

$156 < \mu_B < 420$ MeV

arXiv: 2504.00817



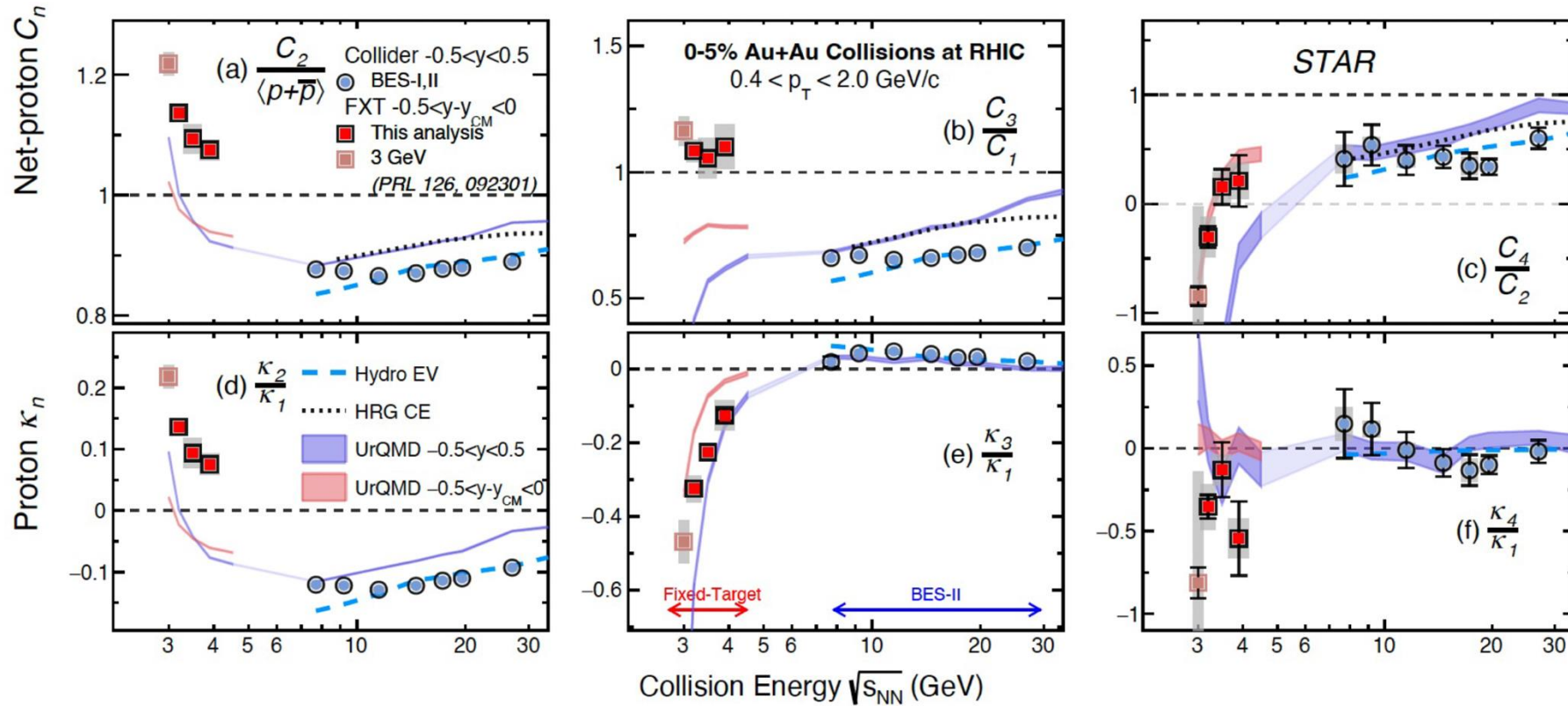
Precision results on net-proton cumulants and proton factorial cumulants from BES-II with greatly improved statistical and systematic uncertainties

**Reduction factor in uncertainties on 0-5% C_4/C_2 :
BES-II vs BES-I**

7.7 GeV		19.6 GeV	
stat. error	sys. error	stat. error	sys. error
4.7	3.2	4.5	4

2 - 5σ deviation from peripheral data or calculations without critical point effects

Net-proton cumulants and proton factorial cumulants from FXT energies



Proton C_4/C_2 , κ_4/κ_1 consistent with UrQMD

Proton (factorial) cumulants deviate from UrQMD at second and third order

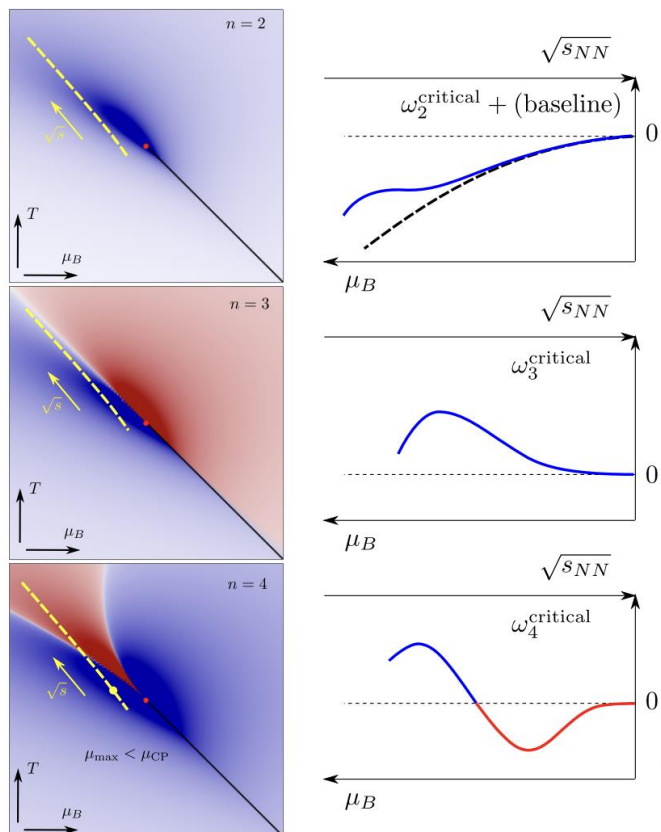
To do:

- Analyze 4.5 GeV and 2B 3 GeV data
- Study rapidity dependence

Proton and anti-proton factorial cumulants from 7.7 GeV to 27 GeV

arXiv: 2504.00817

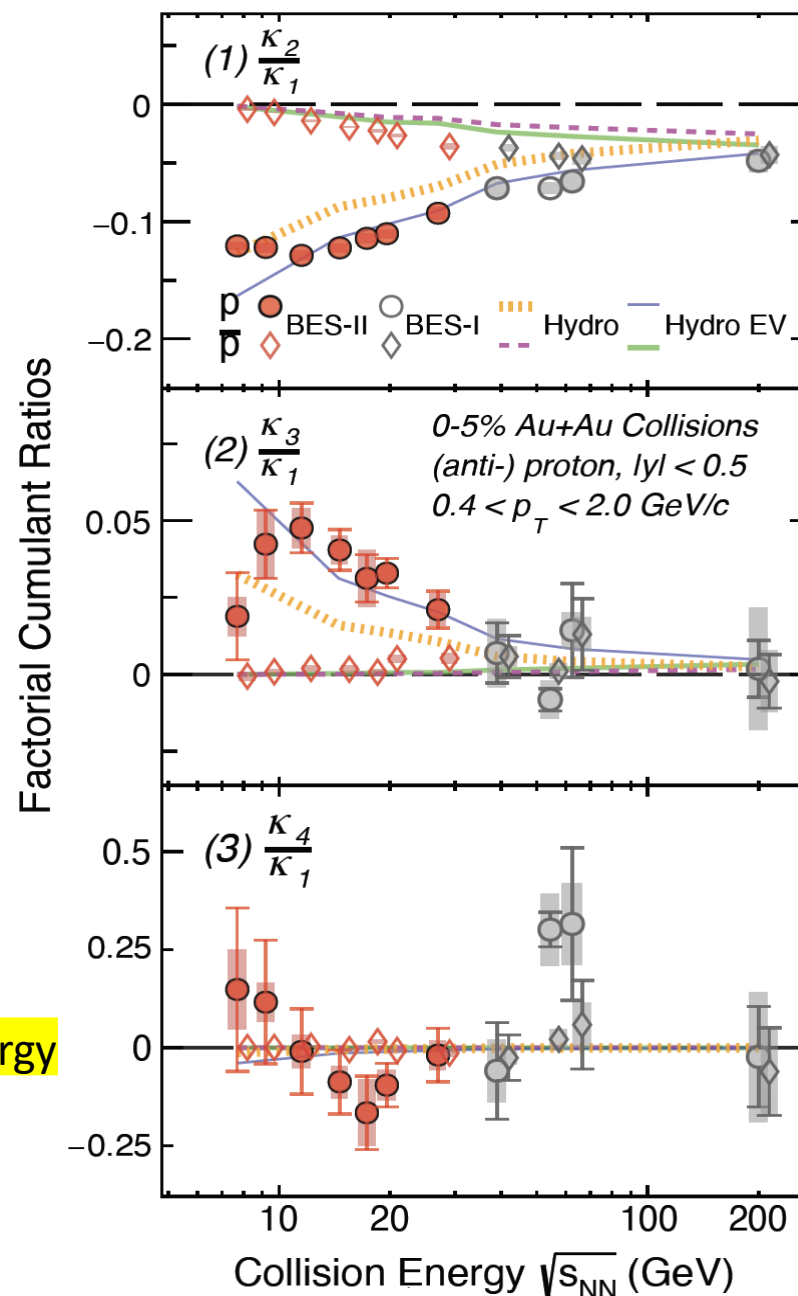
M. Stephanov, arXiv:2410.02861



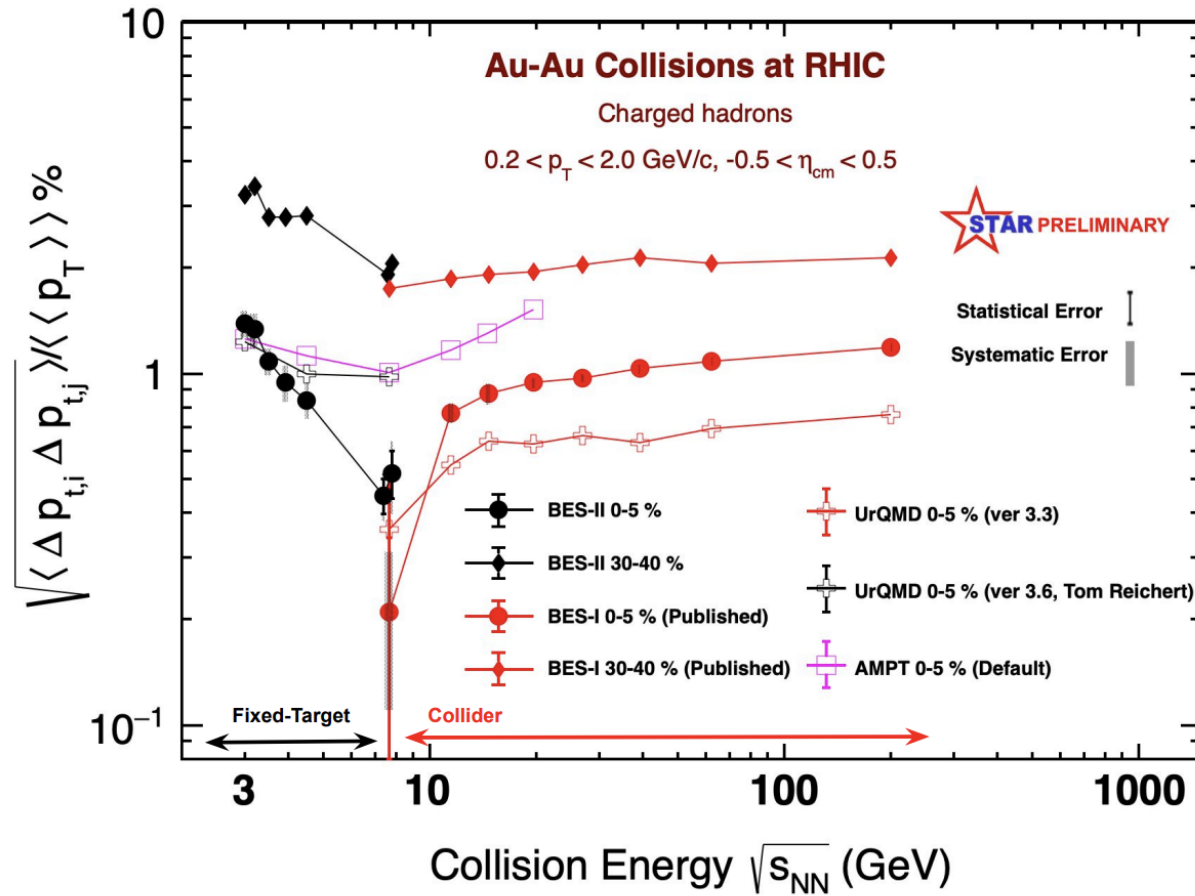
Very interesting trends observed as a function of collision energy

Critical needs:

- Baseline calculations without critical point effects
- Dynamic calculations with critical point effects



Dynamical transverse momentum fluctuations

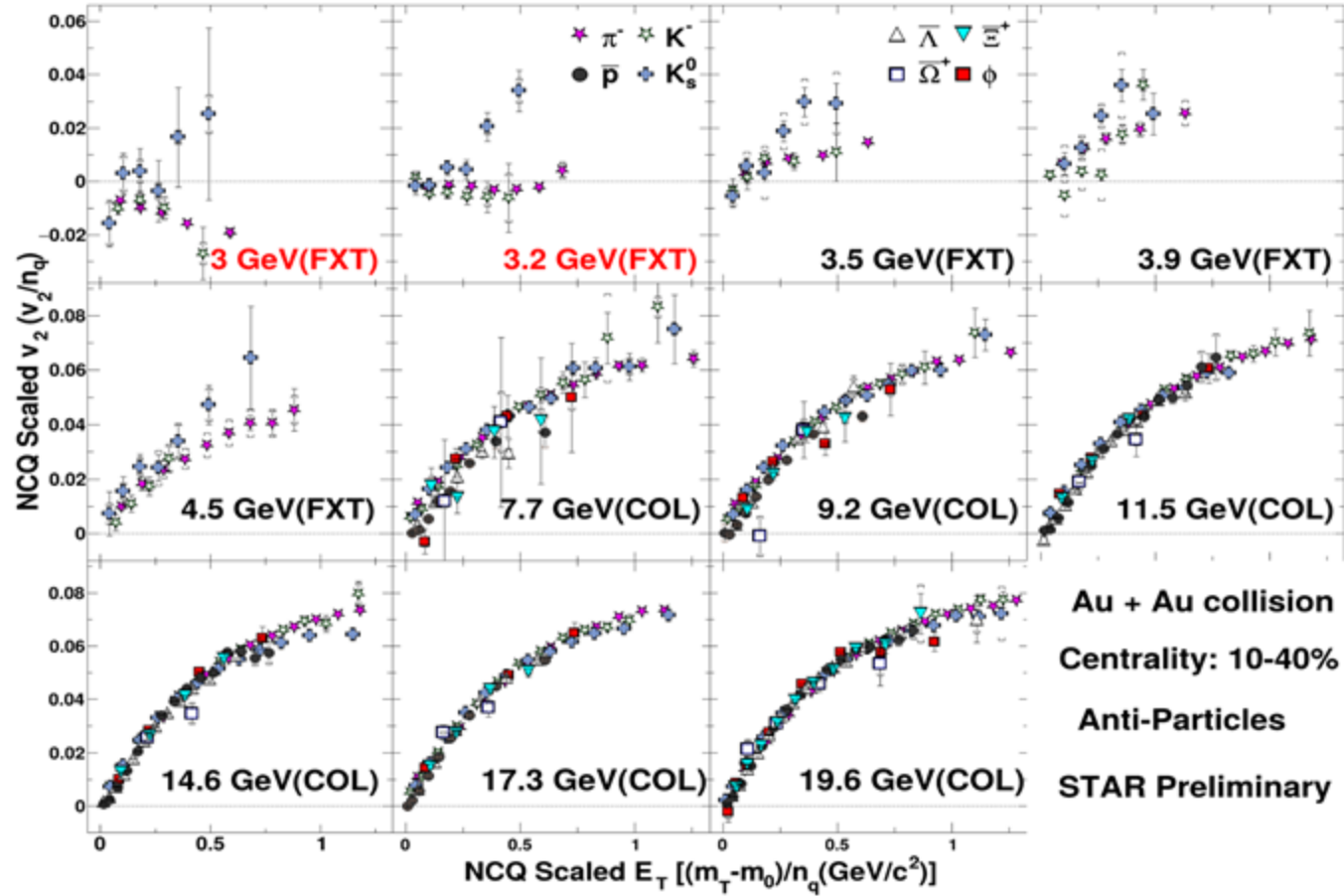


Non-monotonic energy dependence

To do:

- More comprehensive comparisons with baseline models

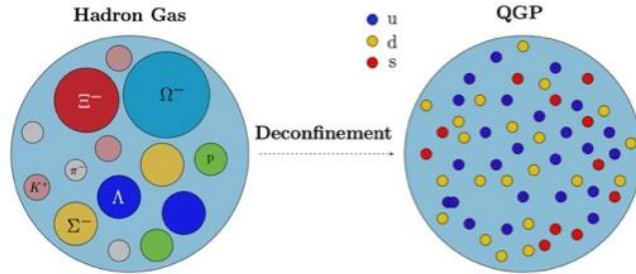
NCQ scaling of elliptic flow



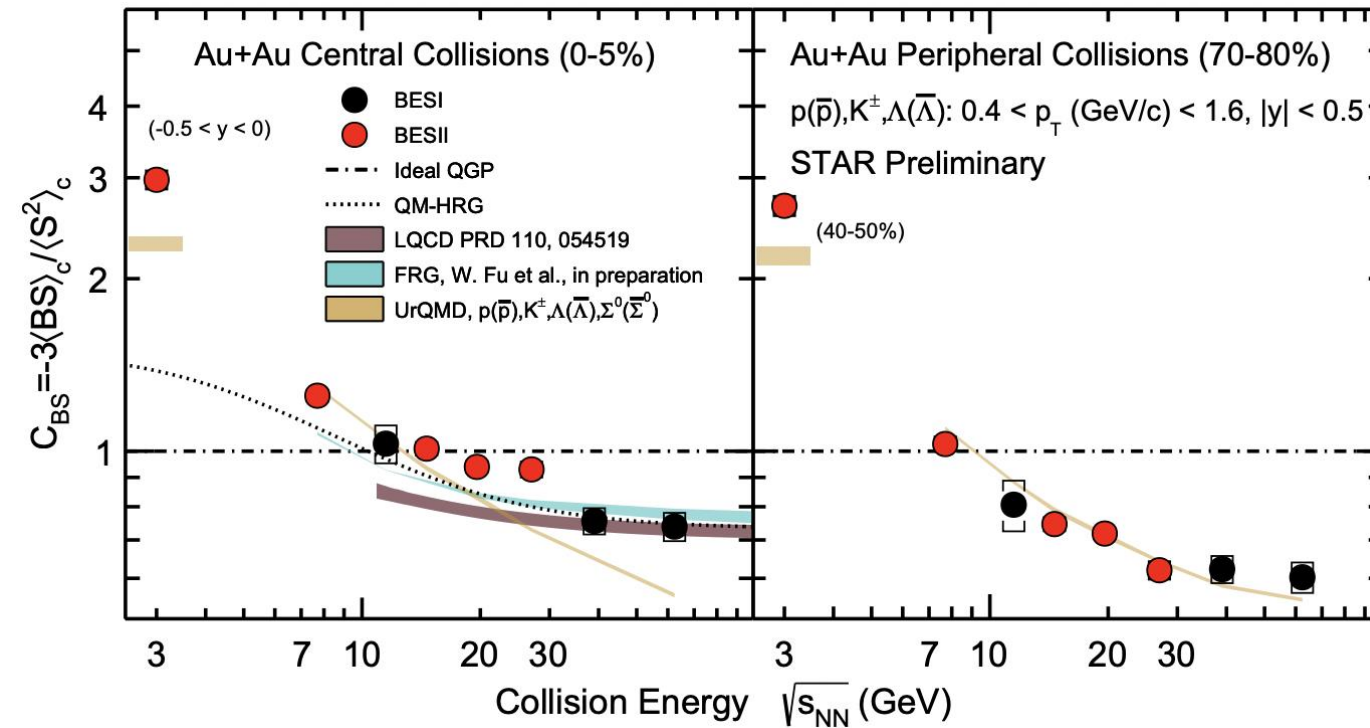
- NCQ scaling holds approximately for 7.7 GeV and above and completely breaks down at 3.2 GeV and below
- Constraints on nuclear shadowing and the onset of partonic collectivity

Baryon-strangeness correlations

Proposed as a sensitive probe of deconfinement

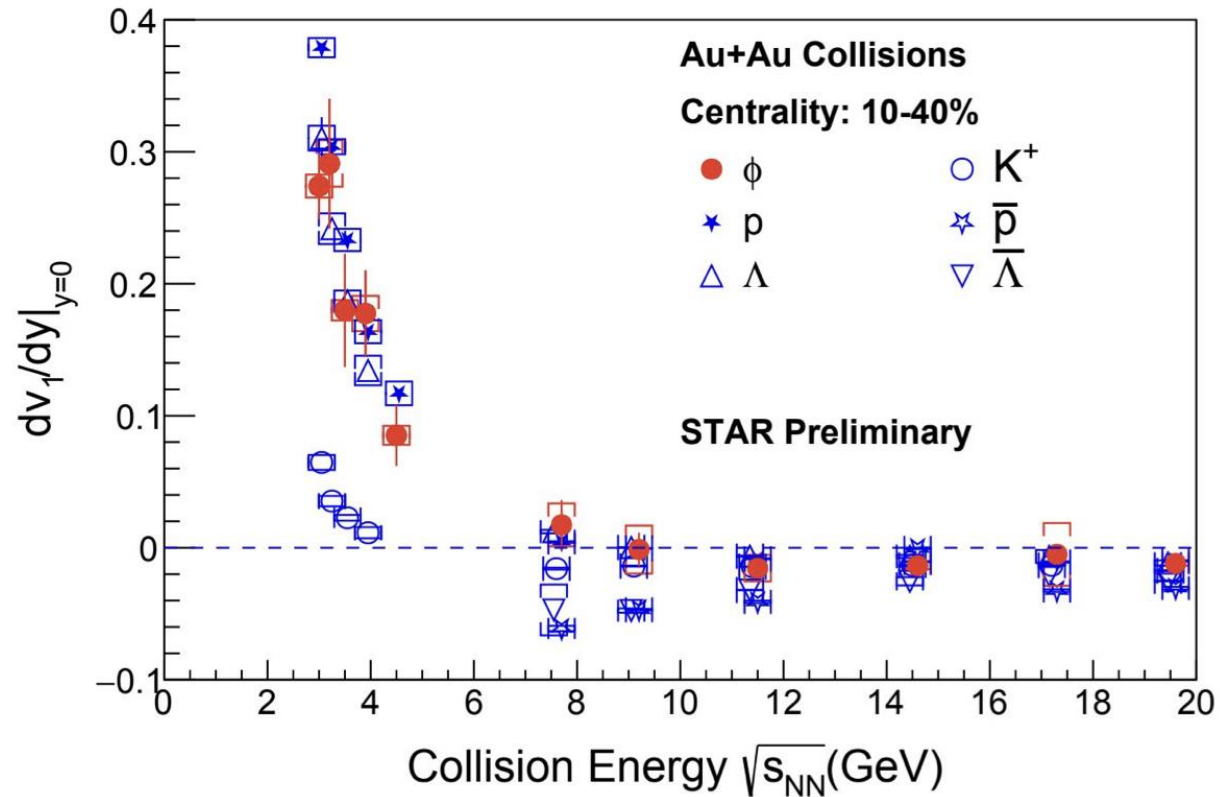


$$C_{BS} = -3 \frac{\langle BS \rangle_c}{\langle S^2 \rangle_c} = -3 \frac{\langle BS \rangle - \langle B \rangle \langle S \rangle}{\langle S^2 \rangle - \langle S \rangle^2}$$



- In peripheral collisions, results are consistent with UrQMD.
- In central collisions, they agree with FRG and LQCD at higher energies, align with UrQMD at lower energies, and deviate from all models in-between.

Directed flow of identified hadrons



Sensitive to the very early stages of the collision

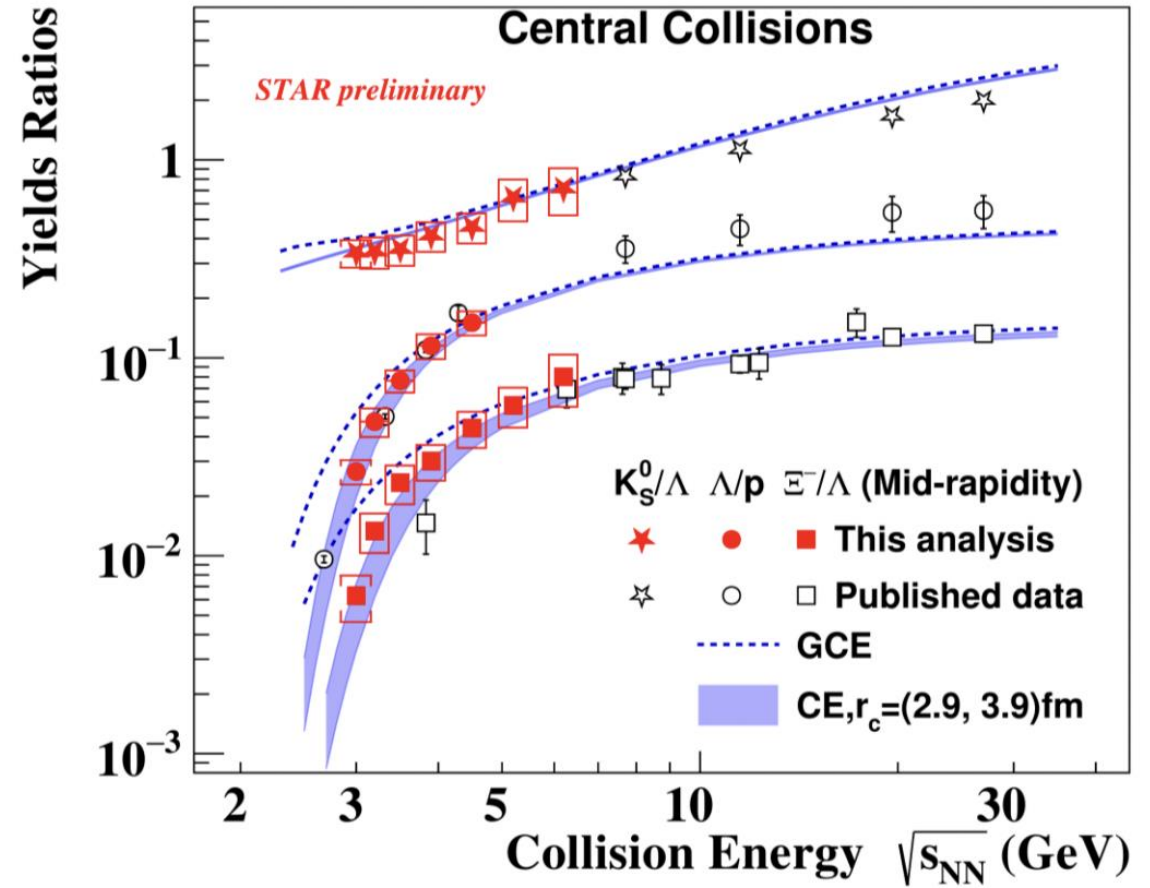
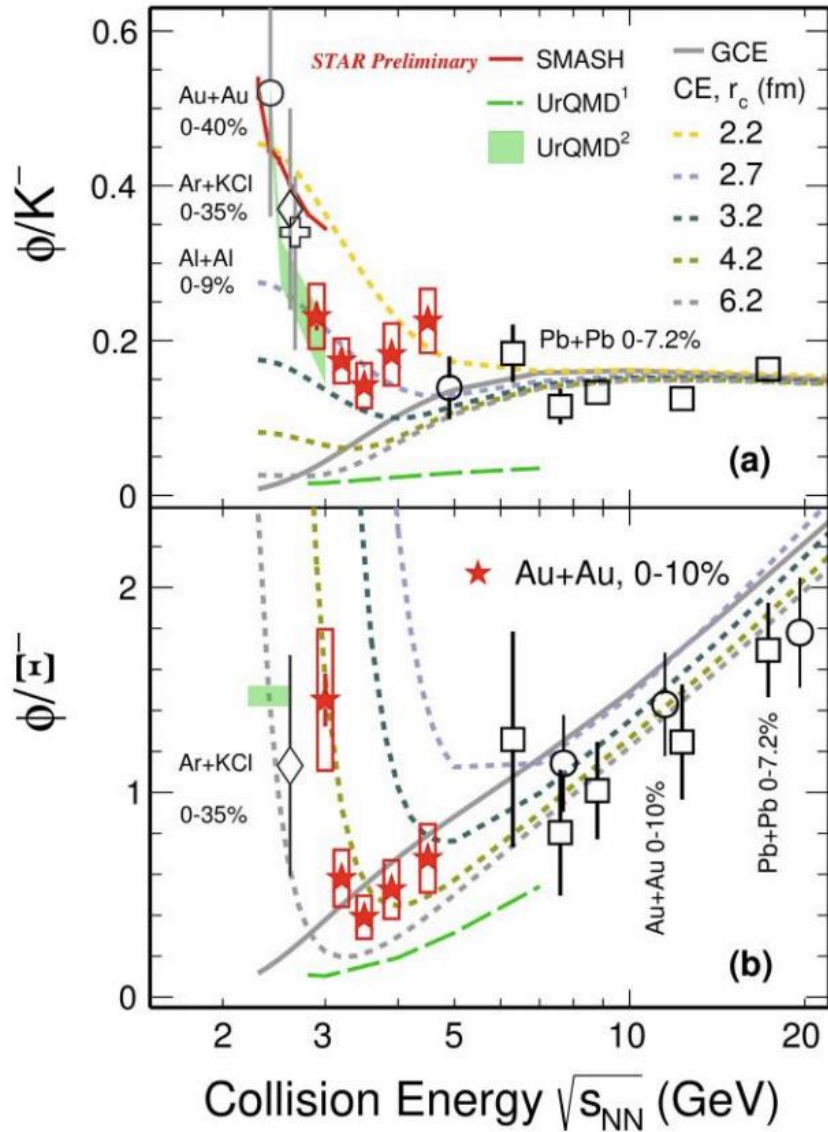
v_1 slope:

- ϕ meson behavior is similar to protons and lambdas
- Matches kaons at 9.2 GeV and above, but shows significant deviations in the FXT energy region

What is the underlying physics mechanism?

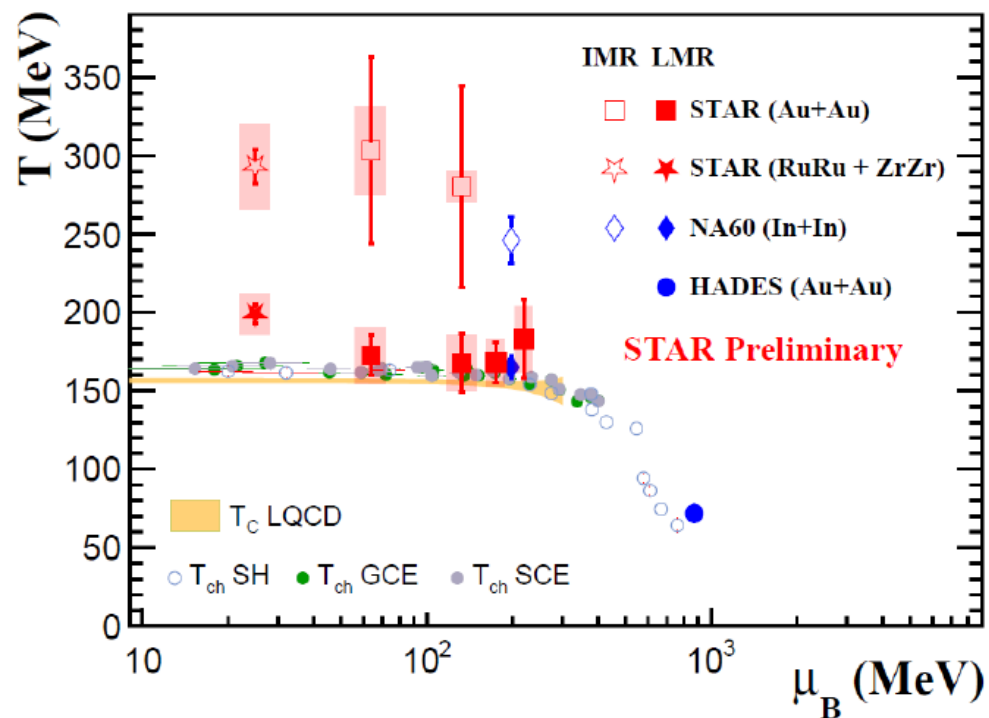
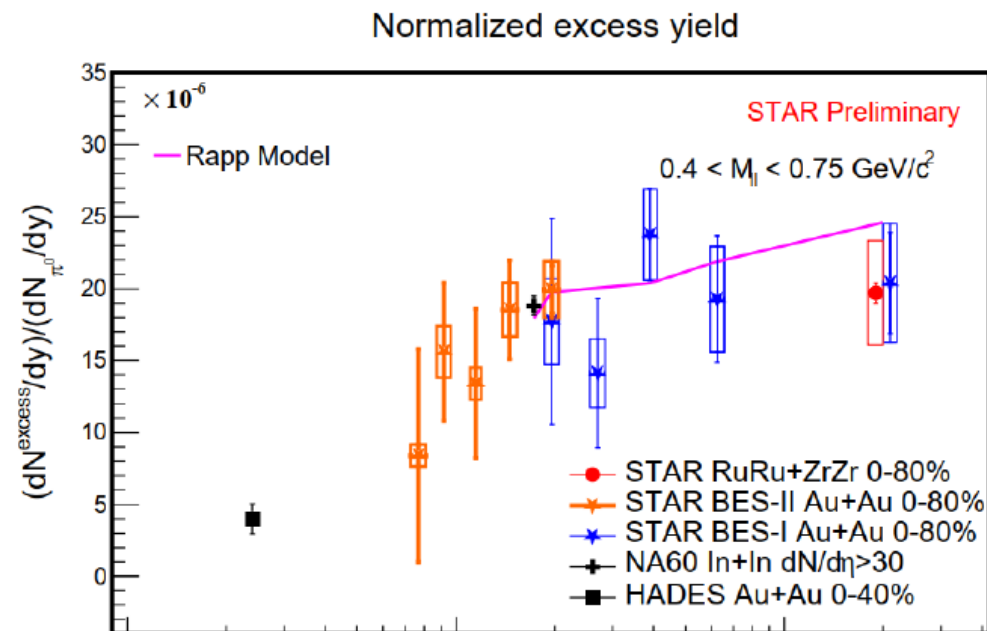
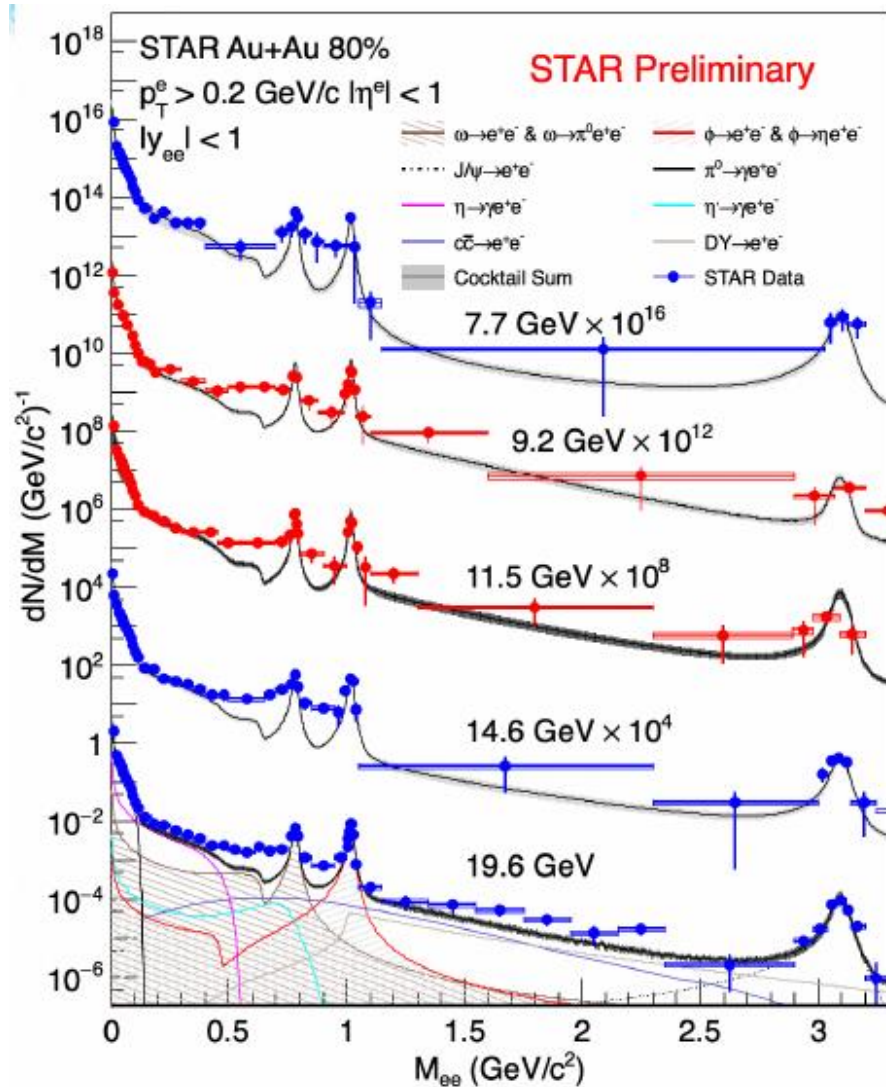
Momentum-dependent mean field potential at lower energies?

Strange hadron production

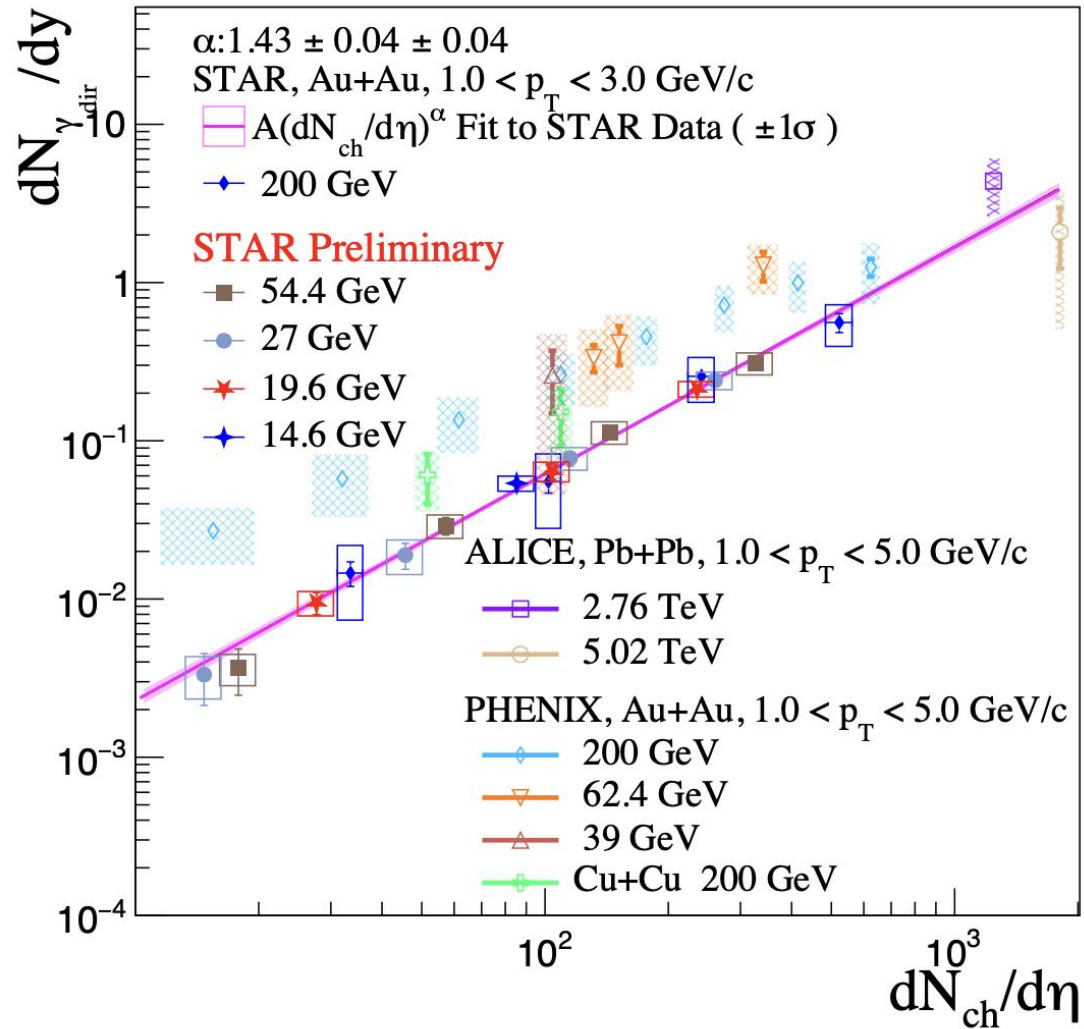


Strange hadron yield ratios deviate from Grand Canonical Ensemble expectations at collision energies below 5 GeV.

Thermal dileptons



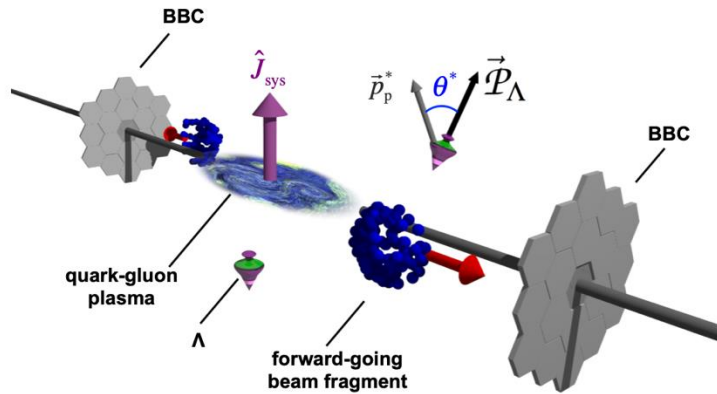
Direct virtual photons



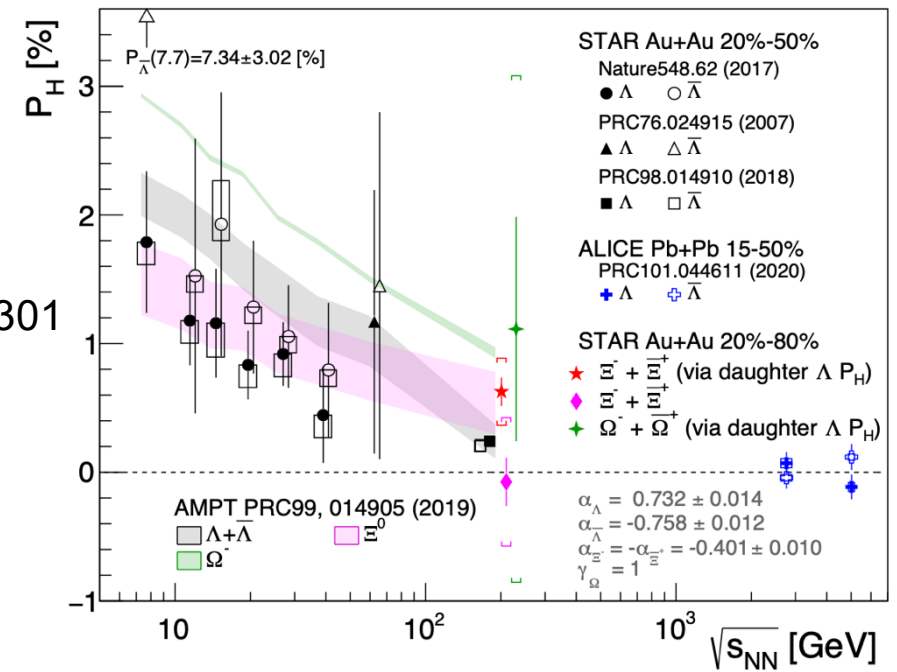
- Yield of direct photons vs. multiplicity from 14.6 to 200 GeV

$$\alpha = 1.43 \pm 0.04 \pm 0.04$$

Hyperon global polarization



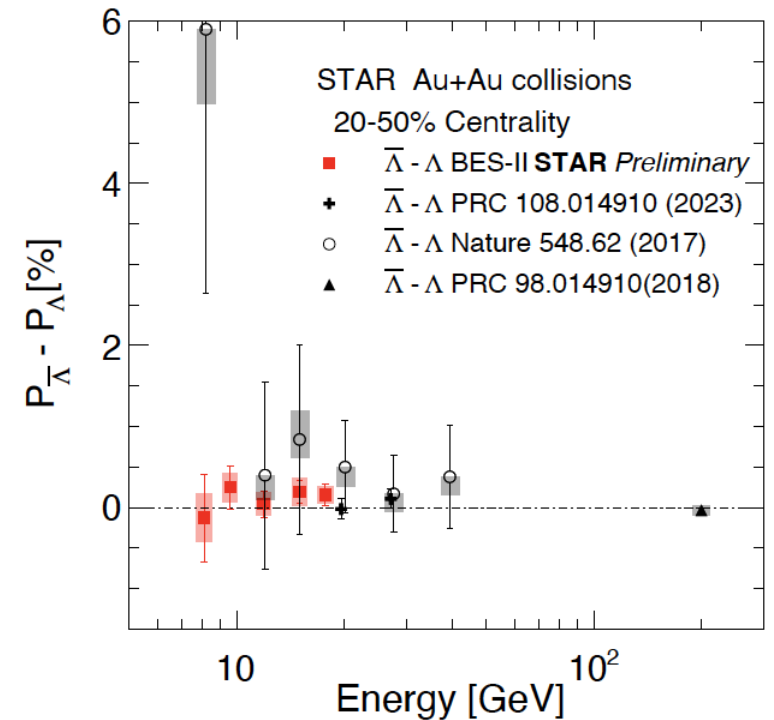
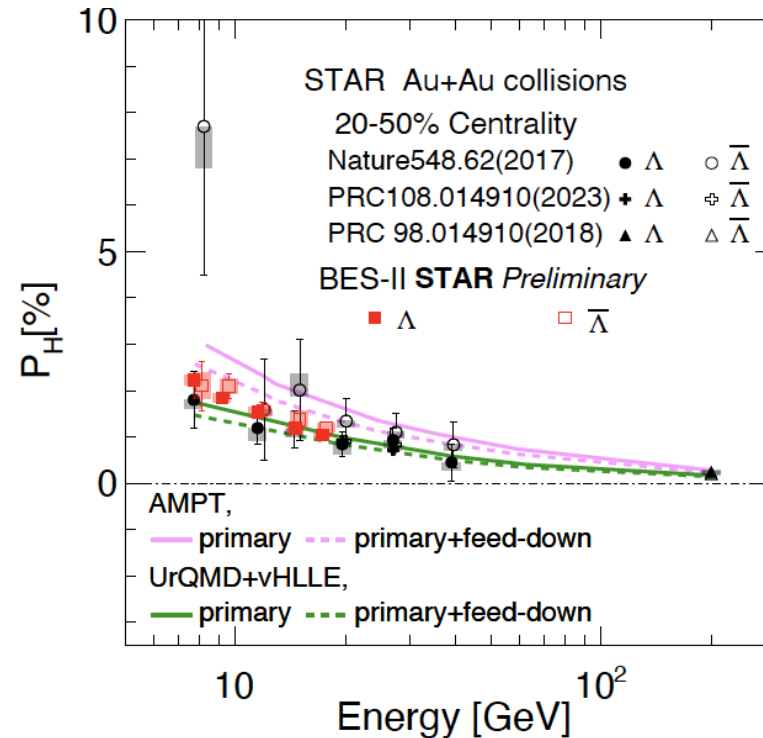
PRL126 (2021) 162301



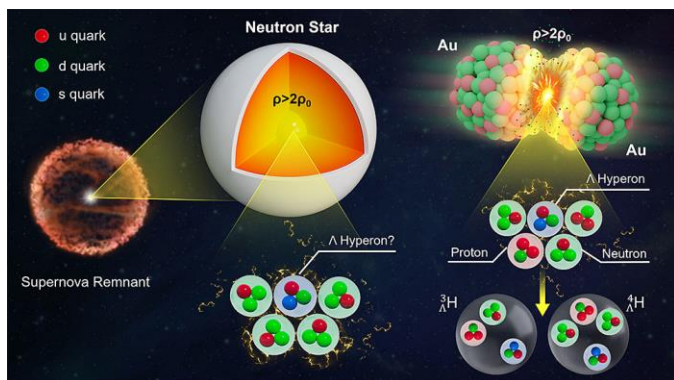
Global angular momentum transfer to hyperon polarization

Heavy ion collisions created the most vortical system ever observed.

Nature **548** (2017) 62

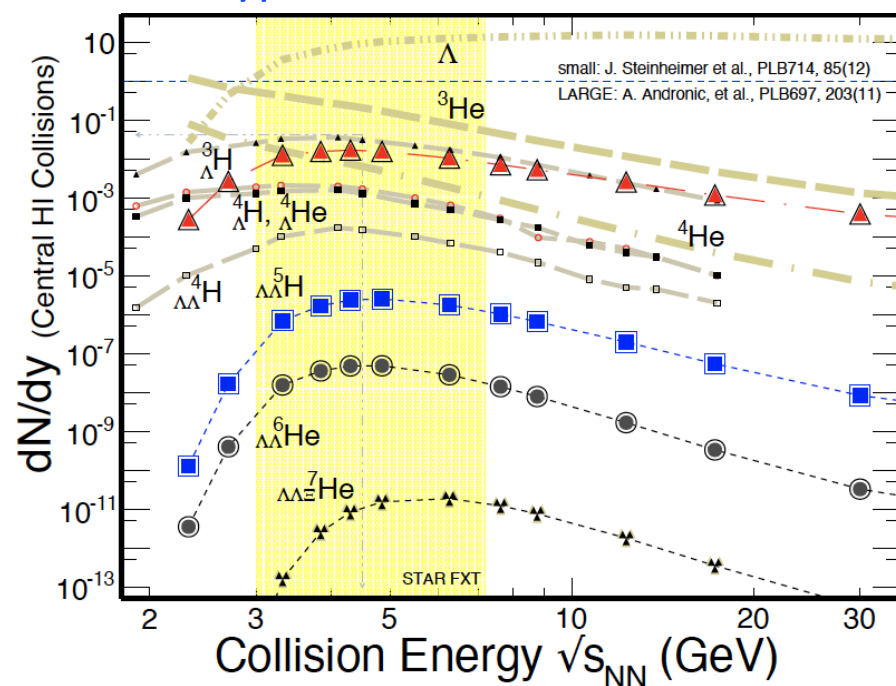


Hypernuclei production

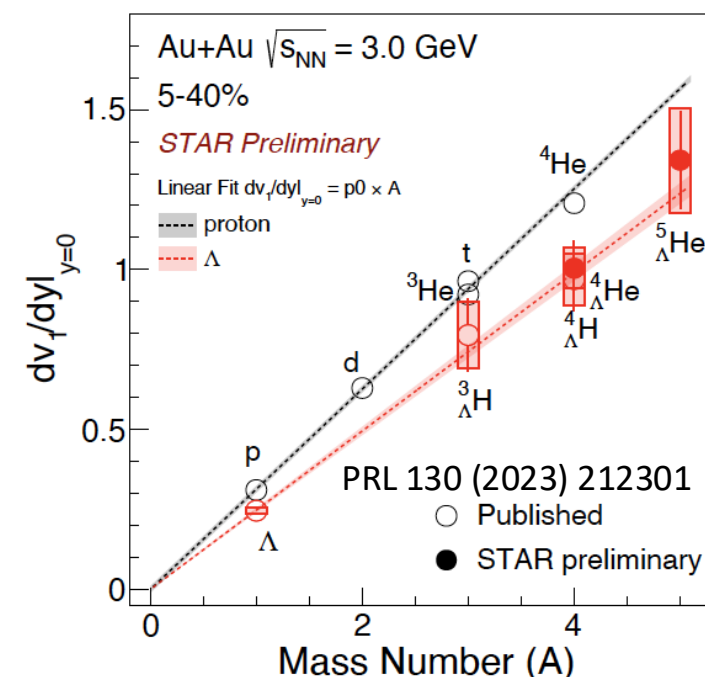
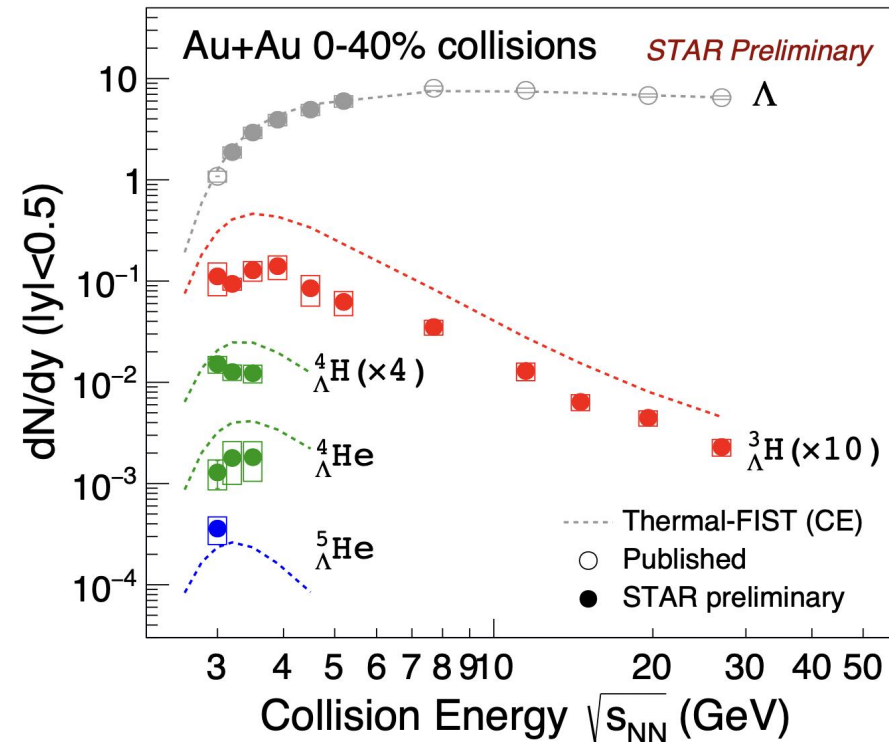


Picture credit:
BNL news article
<https://www.bnl.gov/newsroom/news.php?a=121192>

Hypernuclei Production

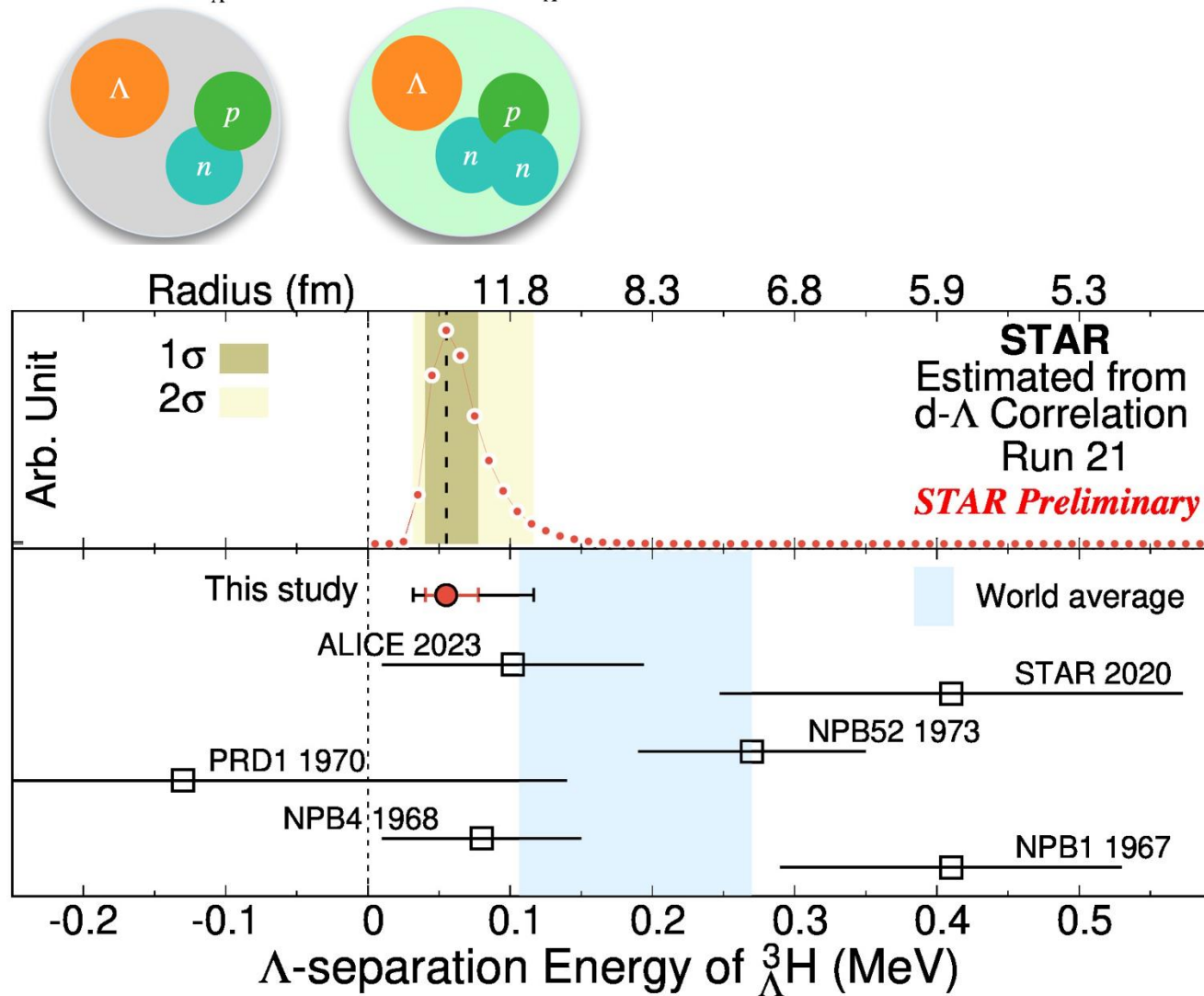


Constrain hyperon – nucleon and hyperon-hyperon interaction
Connection to neutron stars



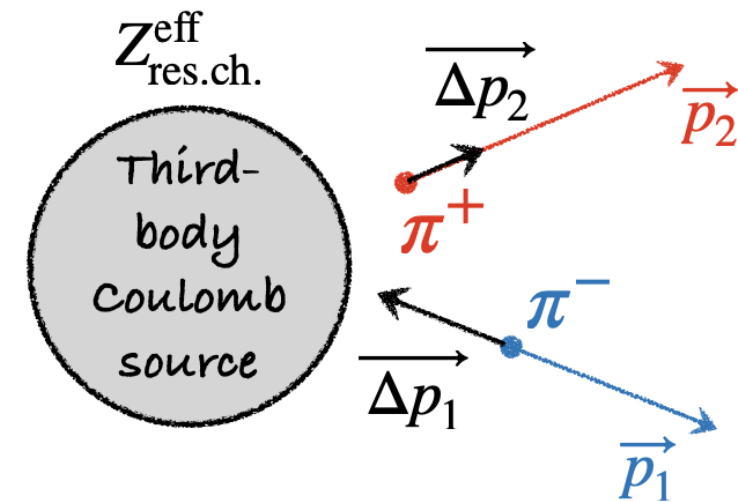
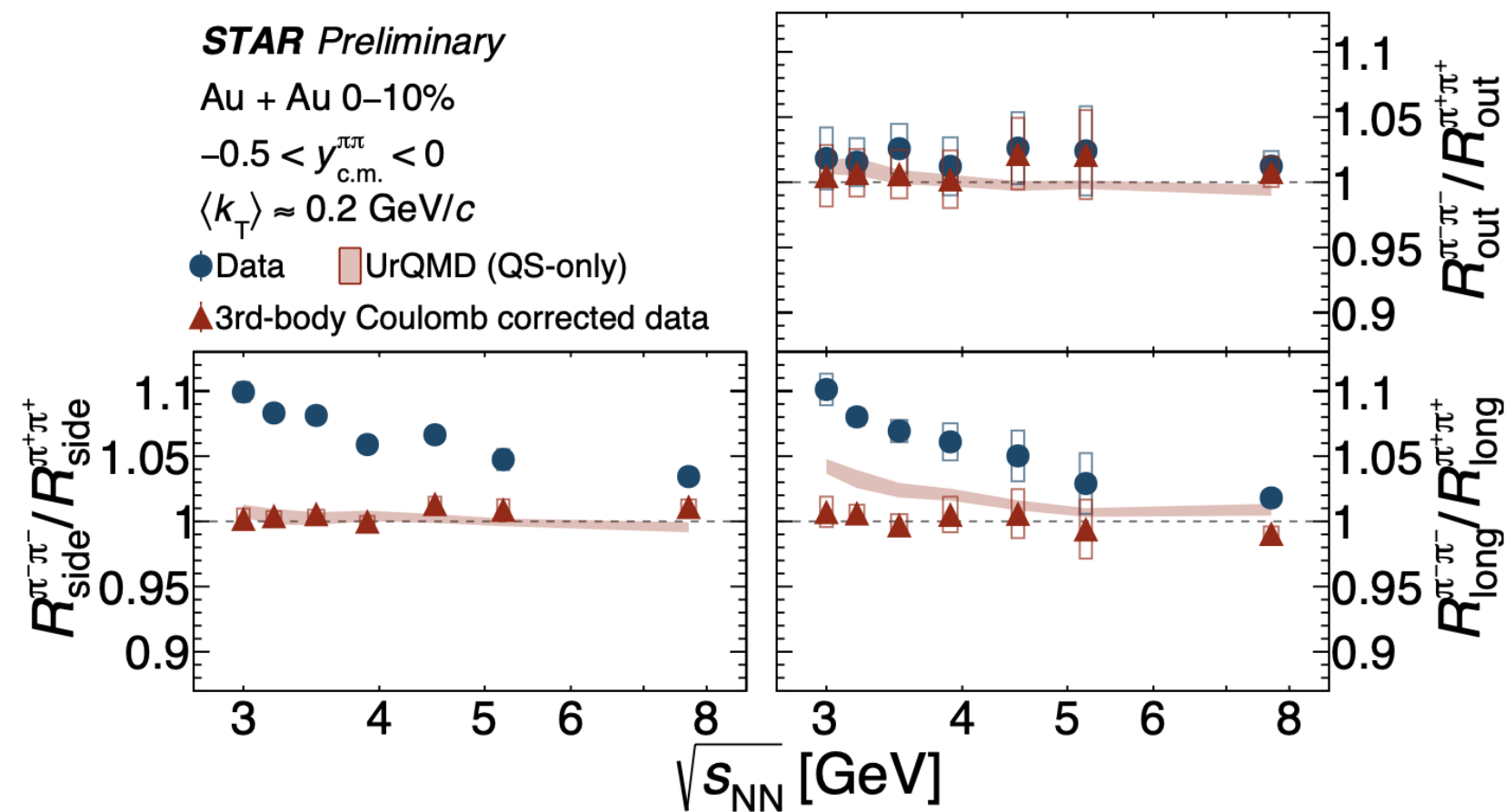
Midrapidity v_1 slopes
follow baryon
number scaling,
implying that
coalescence is the
dominant production
mechanism

Hypernuclei property



- Most precise hypertriton lifetime measurement via d-Lambda correlations
- Measurements of t-Lambda and He3-Lambda correlations ongoing

Third body Coulomb interactions



The measured femtoscopic source radii differ between $\pi^+\pi^+$ and $\pi^-\pi^-$ pairs

- Primarily due to the third-body Coulomb effect.
- No significant isospin effect.

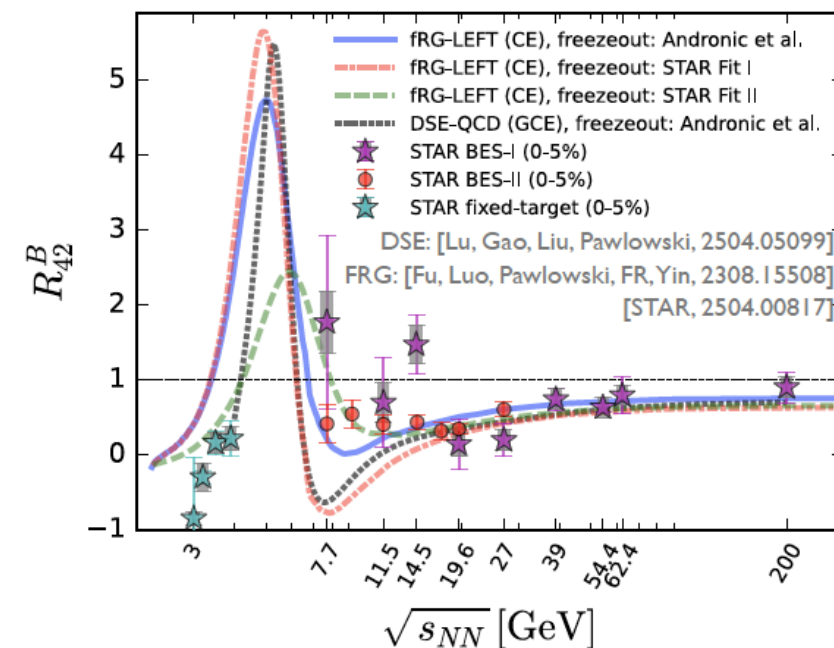
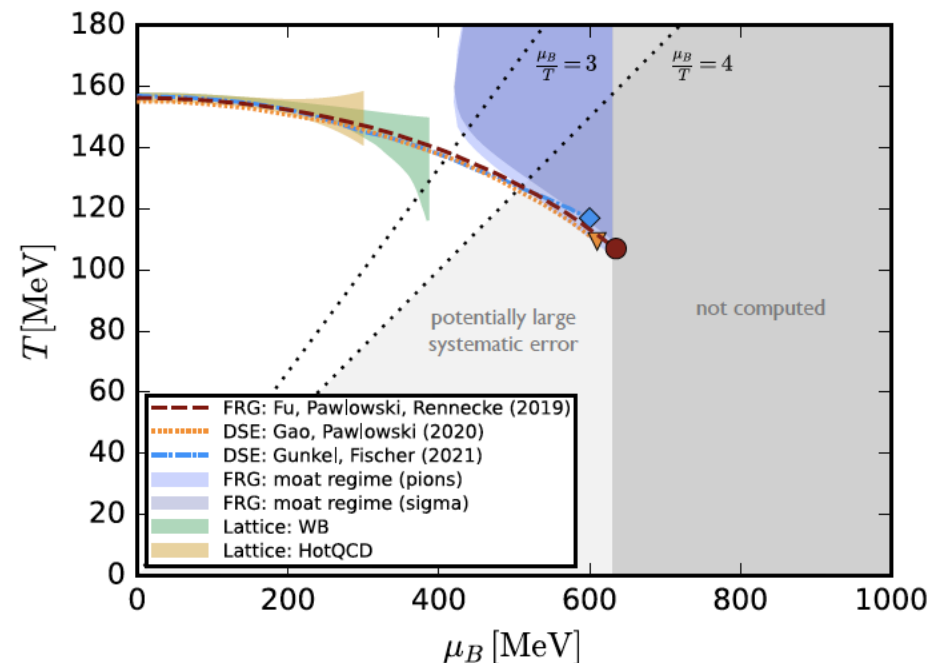
Conclusion

The RHIC BES program has been highly successful, thanks to strong community support and many years of dedicated planning and preparation.

The BES data cover a broad and interesting range of μ_B , enabling us to:

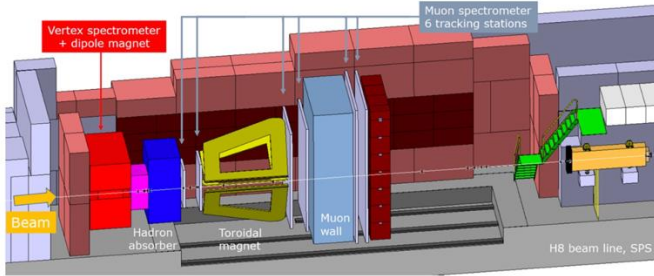
- Search for the QCD critical point
- Explore signatures of a first-order phase transition
- Investigate the onset of QGP formation
- Study hyperon-nucleon interactions
- Examine the vorticity field in heavy-ion collisions
- Measure the freeze-out properties
- ...

Stay tuned—many more exciting results are on the way!

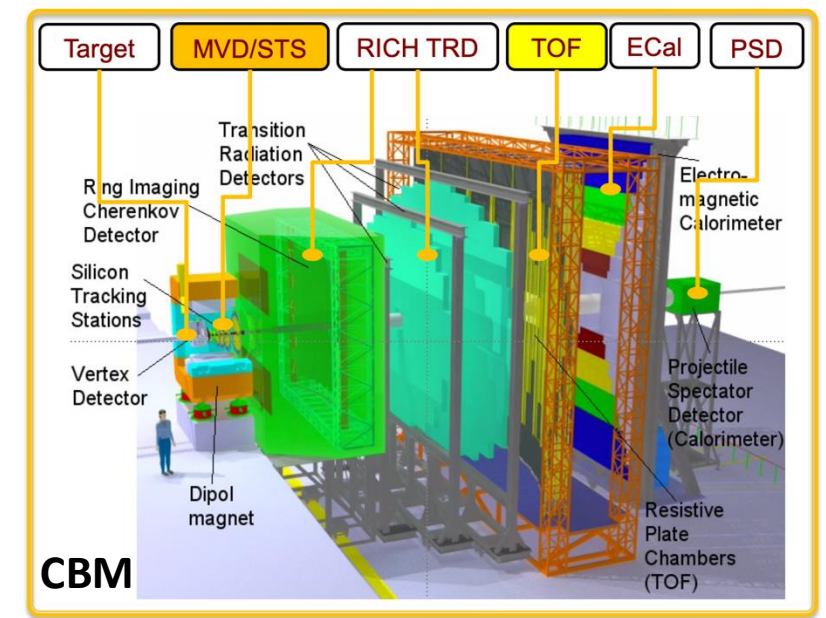
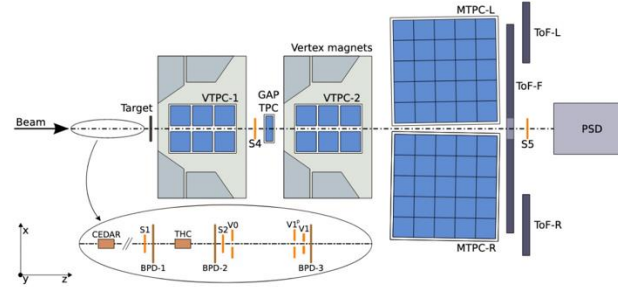


The future

NA60⁺ (2029)

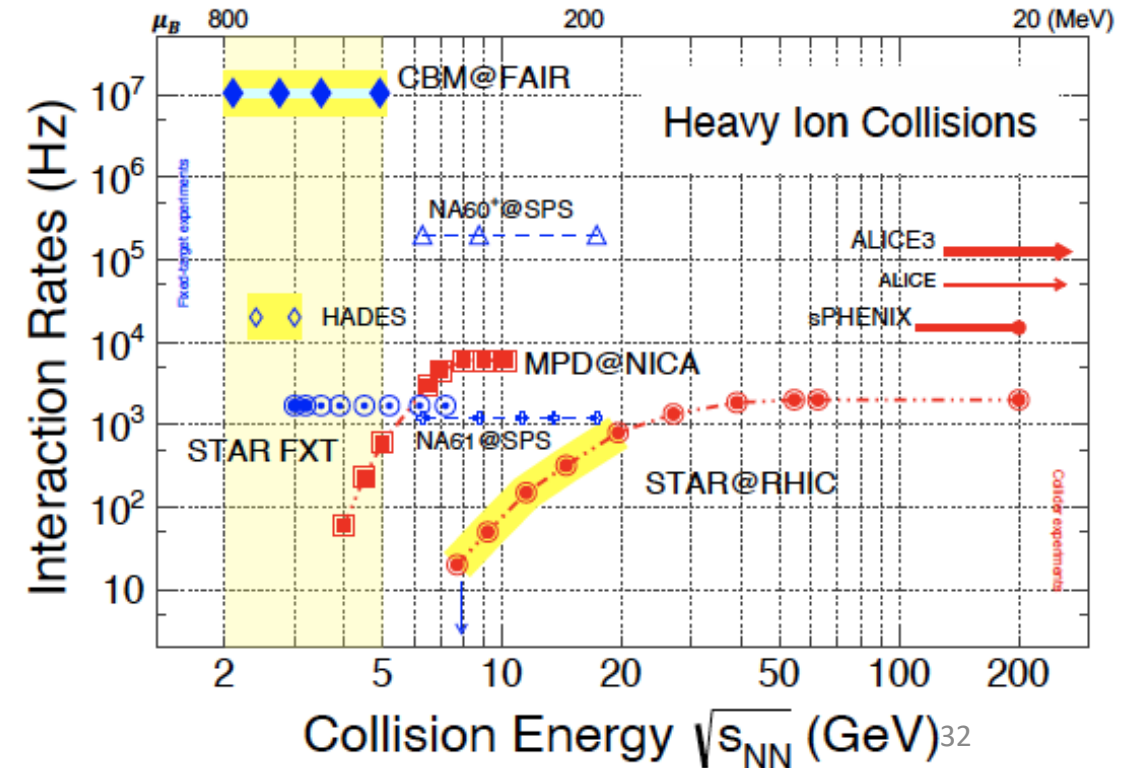


NA61 (2008 - 2027)

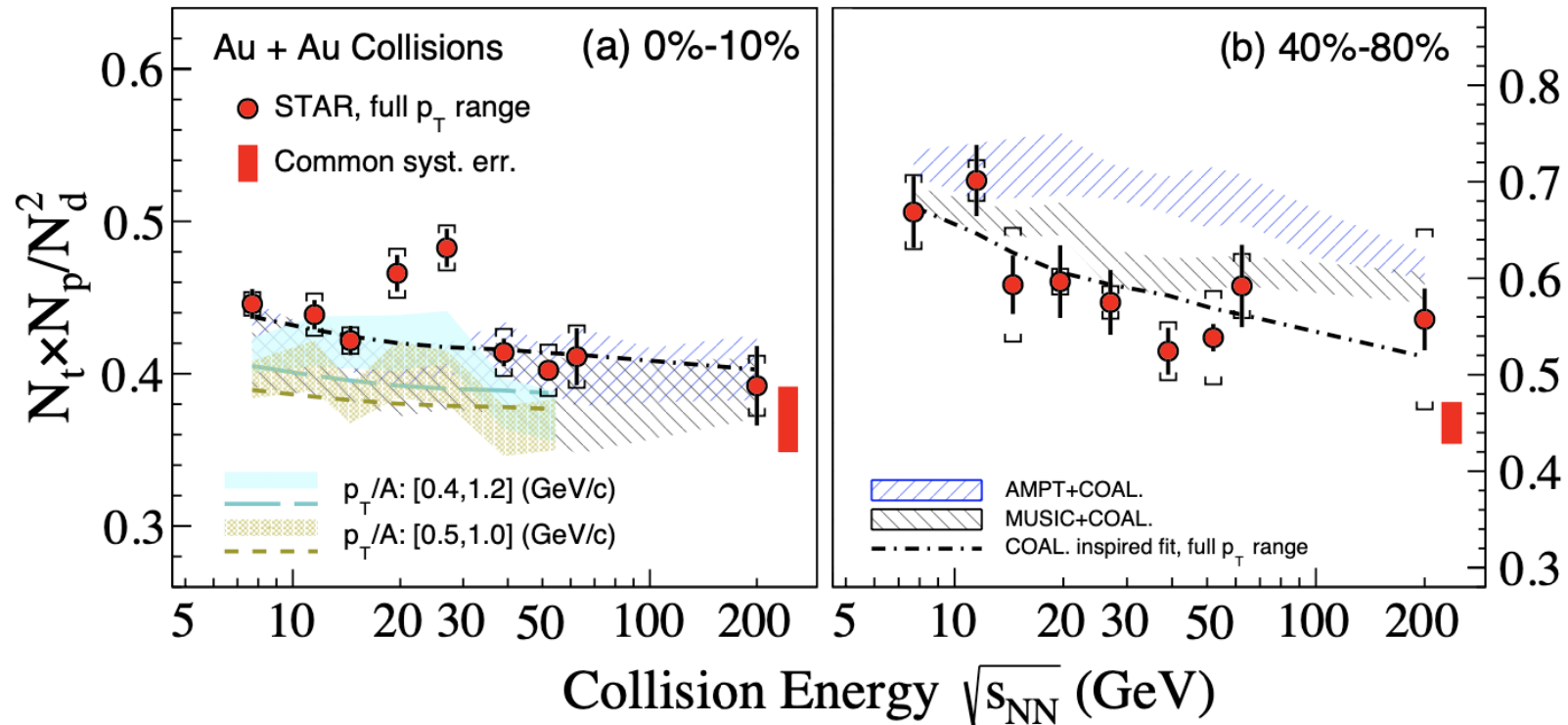


Physics opportunities in the exploration of the QCD phase diagram at high baryon density after the completion of the RHIC BES-II program: NA60+, NA61, CBM, NICA ...

Probe the physics of dense baryon-rich matter and constrain the nuclear equation of state in a regime relevant to binary neutron star mergers and supernovae.



Backup

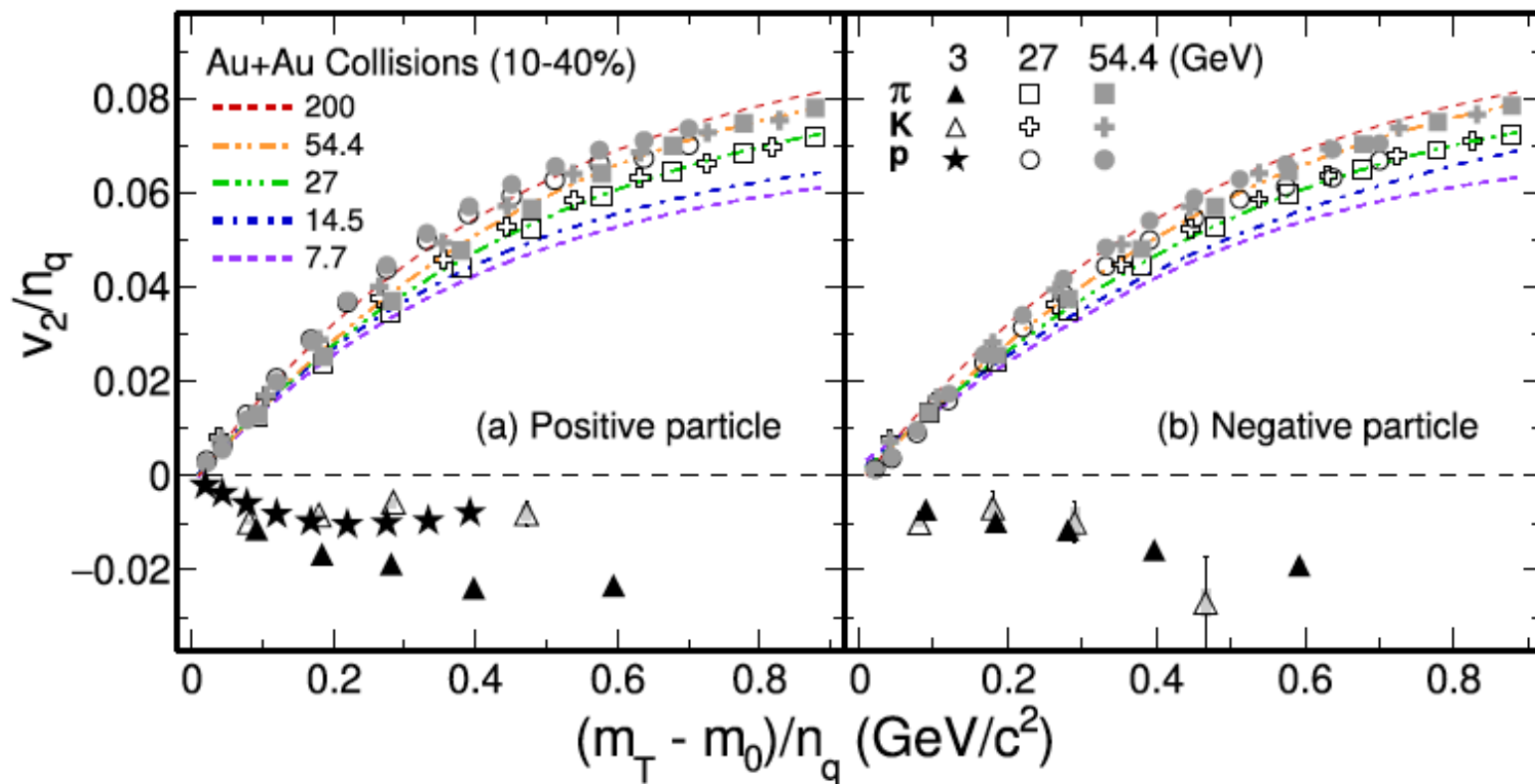


$N_t N_p / N_d^2$, **sensitive to fluctuations of the local neutron density** shows enhancements relative to the coalescence baseline with a significance of 2.3σ and 3.4σ respectively in 0 –10% central Au+Au collisions at 19.6 and 27 GeV.

Constrain production dynamics of light nuclei and understanding of the QCD phase diagram

Disappearance of partonic collectivity in 3 GeV Au+Au collisions

Phys. Lett. B **827** (2022) 137003

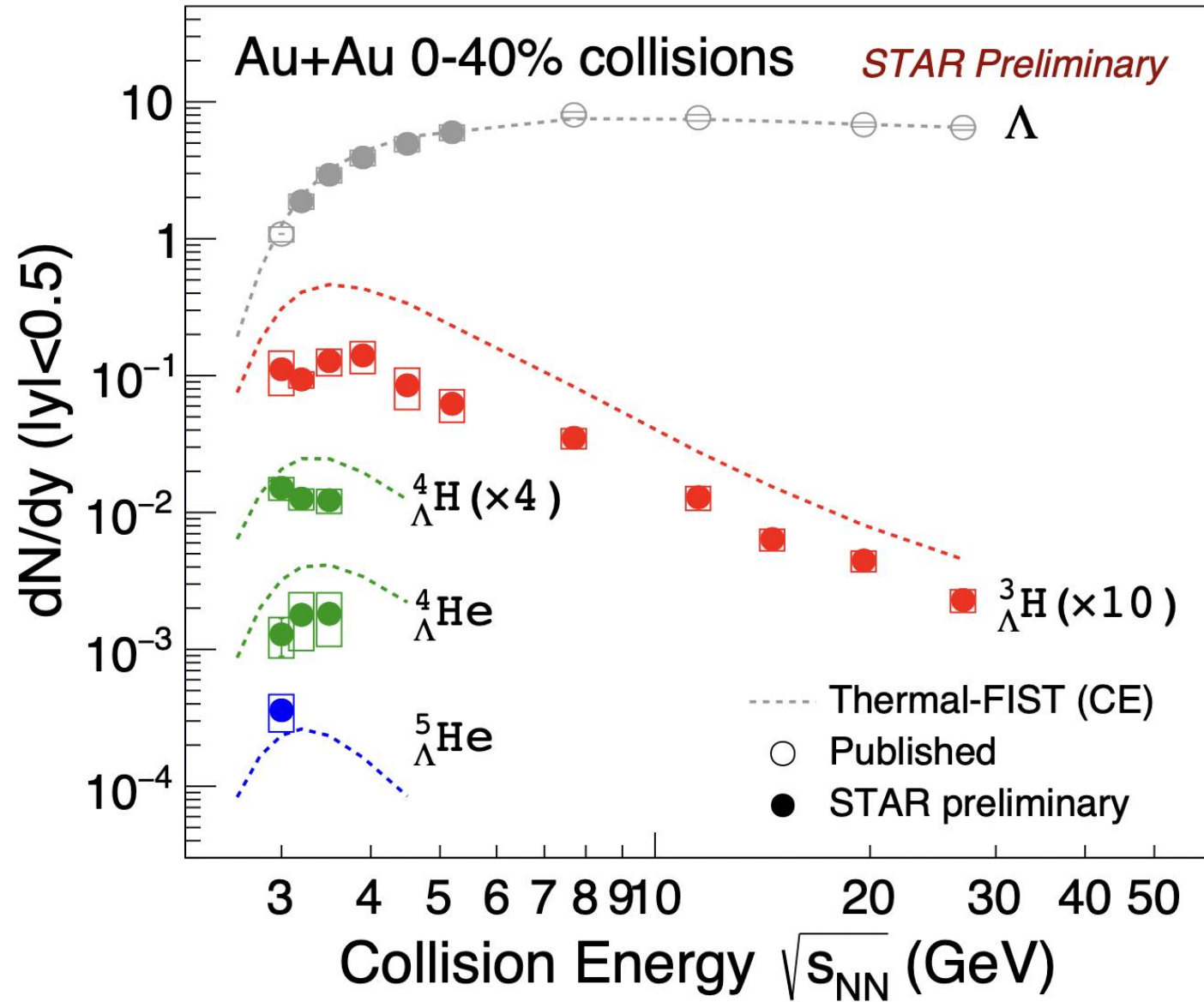
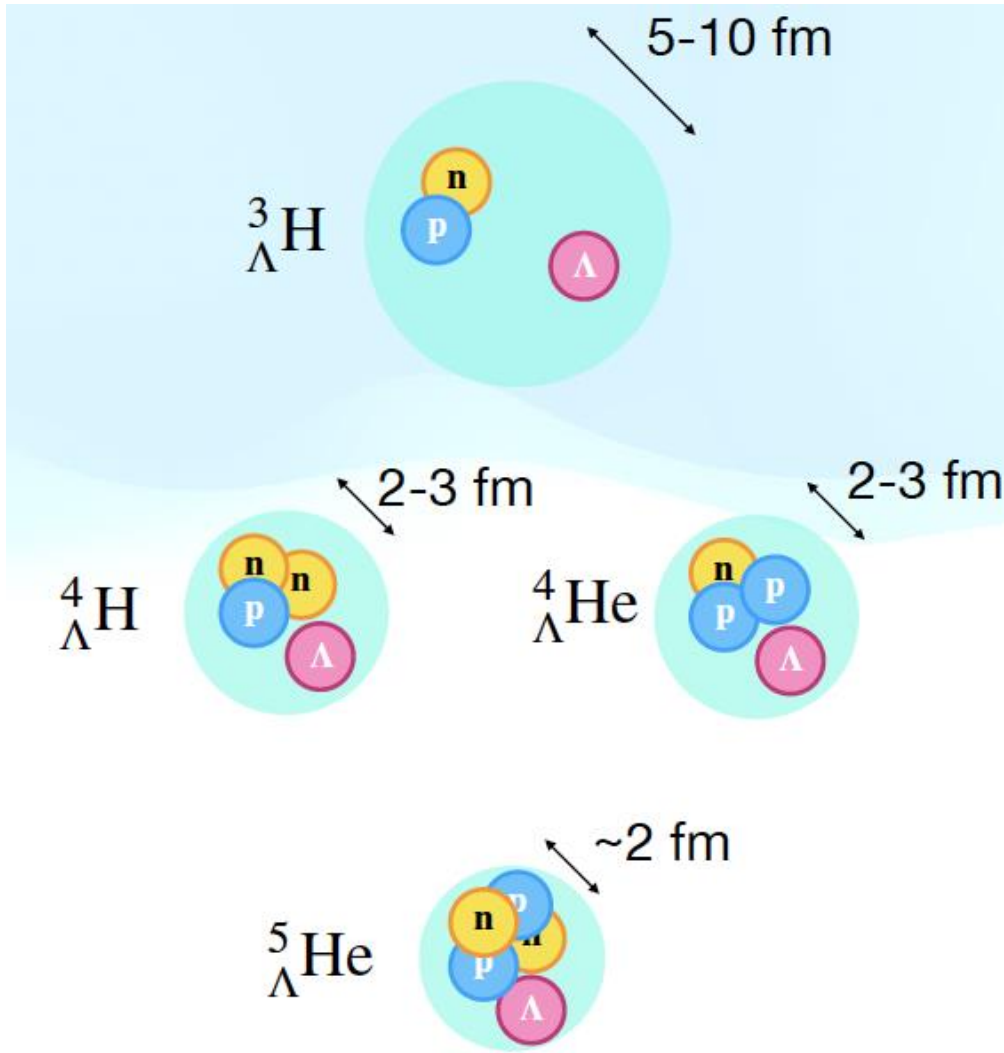


- Number of constituent quark (NCQ) scaling holds at 14.5 GeV and above
- No NCQ scaling and negative elliptic flow observed at 3 GeV

The results can be reproduced with a baryonic mean-field in transport model calculations.

Baryonic interactions dominate in 3 GeV Au+Au collisions

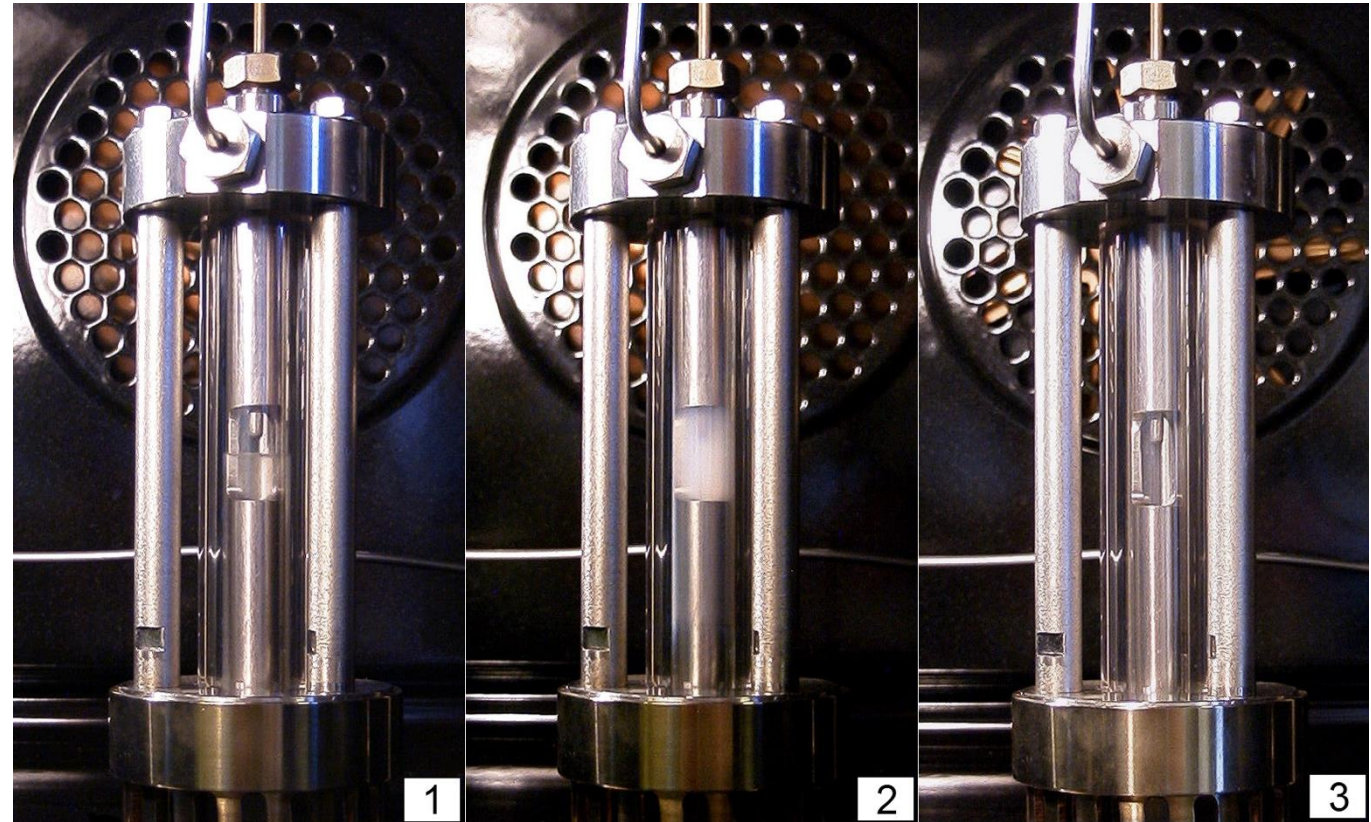
Hypernuclei production



How to infer the QCD critical point

Divergence of the correlation length, dynamics slow down, Large density fluctuations

Critical opalescence, magnetic susceptibility



How to infer the QCD critical point

Correlation length related to various moments of the distributions of conserved quantities such as net-baryon, net-charge, and net-strangeness.

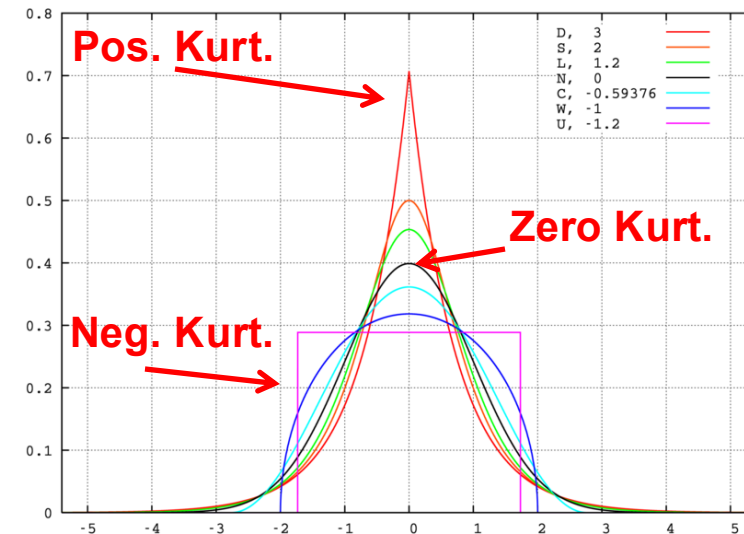
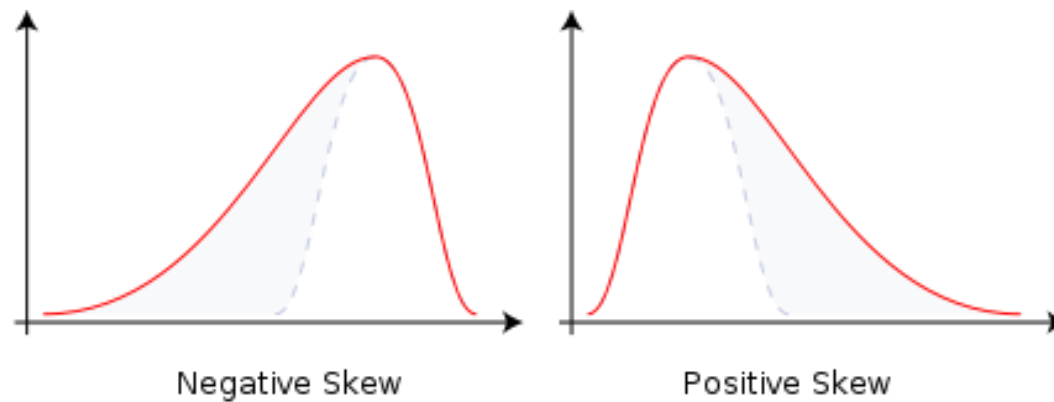
$$\langle (\delta N)^2 \rangle \approx \xi^2, \langle (\delta N)^3 \rangle \approx \xi^{4.5}, \langle (\delta N)^4 \rangle - 3 \langle (\delta N)^2 \rangle^2 \approx \xi^7$$

Mean: $M = \langle N \rangle$

St. Deviation: $\sigma = \sqrt{\langle (N - \langle N \rangle)^2 \rangle}$

Skewness: $S = \frac{\langle (N - \langle N \rangle)^3 \rangle}{\sigma^3}$

Kurtosis: $\kappa = \frac{\langle (N - \langle N \rangle)^4 \rangle}{\sigma^4} - 3$



Measure non-Gaussian fluctuation of conserved quantities

Connection to Lattice QCD

Lattice calculations show that moments of the conserved charge (net-baryon, net-charge, net-strangeness) distributions are related to the susceptibilities

Pressure:

$$\frac{p}{T^4} = \frac{1}{VT^3} \ln Z(V, T, \mu_B, \mu_Q, \mu_S)$$

Susceptibility:

$$\chi_q^{(n)} = \frac{1}{T^4} \frac{\partial^n}{\partial (\mu_q / T)^n} P \left(\frac{T}{T_c}, \frac{\mu_q}{T} \right) \Big|_{T/T_c},$$

$q = B, Q, S$ **(Conserved Quantum Number)**

$$\chi_q^{(1)} = \frac{1}{VT^3} \langle \delta N_q \rangle, \chi_q^{(2)} = \frac{1}{VT^3} \langle (\delta N_q)^2 \rangle$$

$$\chi_q^{(3)} = \frac{1}{VT^3} \langle (\delta N_q)^3 \rangle$$

$$\chi_q^{(4)} = \frac{1}{VT^3} \left(\langle (\delta N_q)^4 \rangle - 3 \langle (\delta N_q)^2 \rangle^2 \right)$$

A. Bazavov et al *arXiv*:1208.1220, 1207.0784.

F. Karsch et al, PLB 695, 136 (2011).

arXiv: 1203.0784; S. Borsanyi et al, JHEP1201,138(2011);